Geology, Geophysics & Environment 2025, vol. 51 (2): 107–132

Continuous contractional deformation followed by extension in the Nowy Sącz Basin, Polish Outer Carpathians: constraints from fault-slip analysis

László Fodor[1], Anna Świerczewska[2], Piotr J. Strzelecki[3]

[1] *HUN-REN Institute of Earth Physics and Space Science, Sopron, Hungary; Eötvös University, Institute of Geography and Earth Sciences, Department of Geology, Budapest, Hungary, e-mail: fodor.laszlo@epss.hun-ren.hu, imre.laszlo.fodor@ttk.elte.hu, ORCID ID: 0000-0002-0606-4414*
[2] *AGH University of Krakow, Faculty of Geology, Geophysics and Environmental Protection, Krakow, Poland, e-mail: swiercze@agh.edu.pl, ORCID ID: 0000-0003-3464-6419*
[3] *AGH University of Krakow, Faculty of Geology, Geophysics and Environmental Protection, Krakow, Poland, e-mail: pjstrzel@agh.edu.pl, ORCID ID: 0000-0003-0102-0719*

Received: 23 October 2024; accepted: 30 December 2024; first published online: 28 May 2025

Abstract: Fault-slip analysis was carried out in the Nowy Sącz Basin and the surroundings of the Polish Outer Carpathians based on field observations, published maps, and publications. A reconstruction of the stress field and the contractional directions from the folds suggests that the area was marked by four different deformation phases, most of them involving several stress states. The tilt test supports the separation of pre-, syn-, and post-folding deformation episodes within the phases which occurred during the folding of the Palaeogene to Early Miocene flysch units and also during the folding of the late Middle Miocene basin fill. After an early extensional phase at the onset of the deformation history, the area was marked by contractional deformation from ~34 Ma to ~8 Ma. During this period the compressional direction did not change markedly but a slight clockwise change of the maximal stress axis may have occurred in the Early Miocene due to vertical-axis block rotation. In this persistent deformation field, the basin could have had a contractional origin in front of an out-of-sequence thrust. The latest Miocene(?) to Quaternary deformation was probably related to the extensional collapse of the Carpathian accretionary wedge.

Keywords: fault-slip analysis, Neogene, Quaternary, Outer Carpathians, folding, thrust

INTRODUCTION

Small sedimentary basins are scattered all along the East Alpine–Carpathian–Dinaric orogenic belt. These basins, often referred to as "intramountain basins", represent the late-stage evolution of the fold-and-thrust belts but the time span which elapsed between the main thrusting and the basin formation varies from place to place. Similarly, their tectonic origin is variable. Intramountain basins of the easternmost Alps are mostly attributed to Neogene strike-slip faulting (Ratschbacher et al. 1991, Sachsenhofer et al. 2000, Gruber et al. 2004), and are connected to the eastward extrusion of the Alpine nappe pile (Ratschbacher et al. 1989) although a late-stage contractional overprint also occurred in some basins (Nemes et al. 1997, Sachsenhofer et al. 2000, Gruber et al. 2004).

https://doi.org/10.7494/geol.2025.51.2.107 ISSN 2299-8004 | e-ISSN 2353-0790 | Wydawnictwa AGH

Several basins of the Dinarides have an extensional origin already related to the late-stage extensional collapse phase (Andrić et al. 2017, Porkoláb et al. 2019). Basins in the south-eastern bend area of the Carpathians are superimposed on the volcanic chain and post-date the main frontal thrusting of the Carpathians. Thus, their formation could be related to deep processes at work beneath the orogen, in the mantle lithosphere and/or mantle wedge (Fielitz & Seghedi 2005). These examples show that the tectonic origin of intramountain basins should be clarified because they contain information about the late-stage tectonic evolution of the orogen or already their destruction by successive deformation phases.

The fold-and-thrust belt of the Outer Western Carpathians in Poland and Slovakia was covered by Middle Miocene sediments which are preserved in several "intramountain" basins, the two largest being the Orava-Nowy Targ and Nowy Sącz basins (ONT and NS basins, respectively). Despite the poor outcrop conditions of the Middle Miocene sediments, several structural studies based on joints and faults have been carried out in recent last years in the ONTB (e.g., Struska 2008, Łoziński et al. 2015, Ludwiniak et al. 2019). In the NSB, the study of fractured pebbles from Miocene and Quaternary formations, and fracture analysis in the flysch units has been carried out (Tokarski et al. 2006, 2020). Based on these works, geological mapping, and stratigraphic evolution, earlier suggestions for the origin of the NSB vary from extensional through collapse or compressional origin (see summary of Oszczypko-Clowes et al. 2009), so its structural character and its role in the evolution of the Outer Carpathians remained undetermined.

In this contribution, we present field structural observations of all types of fractures including fractured pebbles and deformation bands and the derived fault-slip analysis, from the poorly exposed Middle Miocene basin fill and from Paleogene to Early Miocene rocks from the basin rims. These structural data can be compared to earlier fault-slip analyses and to the main tectonic phases of the orogen, including frontal accretion and hinterland back-thrusting within the orogenic wedge. The analyses suggest an evolution from a quasi-continuous contractional deformation during the orogen building to extensional deformation after the cessation of the main frontal thrusting. The late-stage extension, apparently showing a bidirectional character, can be connected to a collapse of the orogenic wedge documented already by Tokarski et al. (2012, 2024).

GEOLOGICAL SETTING

The Outer Western Carpathians represent a thrust and fold belt which, as with many other examples worldwide, was gradually accreted in sequence (Oszczypko 1998, 2006, Golonka et al. 2005, Nemčok et al. 2006). In the early part of the deformation history, syn-tectonic sediments dominantly comprised the deep marine flysch sequences, while bathyal to marginal marine sediments infilling the foredeep basin gradually covered the down-bending European plate in the later stage of its evolution (Fig. 1) (Oszczypko et al. 2006, Oszczypko & Oszczypko-Clowes 2012). The in-sequence deformation might have started before the onset of folding, at least this is suggested by the formation of deformation bands prior to complete lithification and maximum burial (Tokarski & Świerczewska 1998, Strzelecki et. al. 2021, Strzelecki & Świerczewska 2023). The folding and nappe stacking process was accomplished from the Paleogene onward, while an important phase of the accretion of foreland sediments happened during the Middle to early Late Miocene (Wójcik et al. 1999, Oszczypko et al. 2006, Gągała et al. 2012, Krzywiec et al. 2012). Frontal thrusting was ongoing up to the early Late Miocene (Wójcik & Jugowiec 1998, Krzywiec et al. 2014, Wójcik et al. 2021), while the outer foredeep sediments were deformed even later (Rauch 2009, Márton et al. 2011). Some parts of the Outer Carpathians remained active during the Quaternary (Zuchiewicz et al. 2009, Tokarski et al. 2020) while the recent stress field is still compressional (Jarosiński 2006).

In the intramountain Nowy Sącz Basin, overlying the flysch belt, sedimentation started with the deposition of the basal terrestrial clastics attributed to the Biegonice Formation (Fig. 2) (Oszczypko et al. 1991). This was followed by predominantly fine-grained, shallow marine sedimentation of the Iwkova and Niskowa formations (Oszczypko et al. 1992, Oszczypko-Clowes et al. 2009).

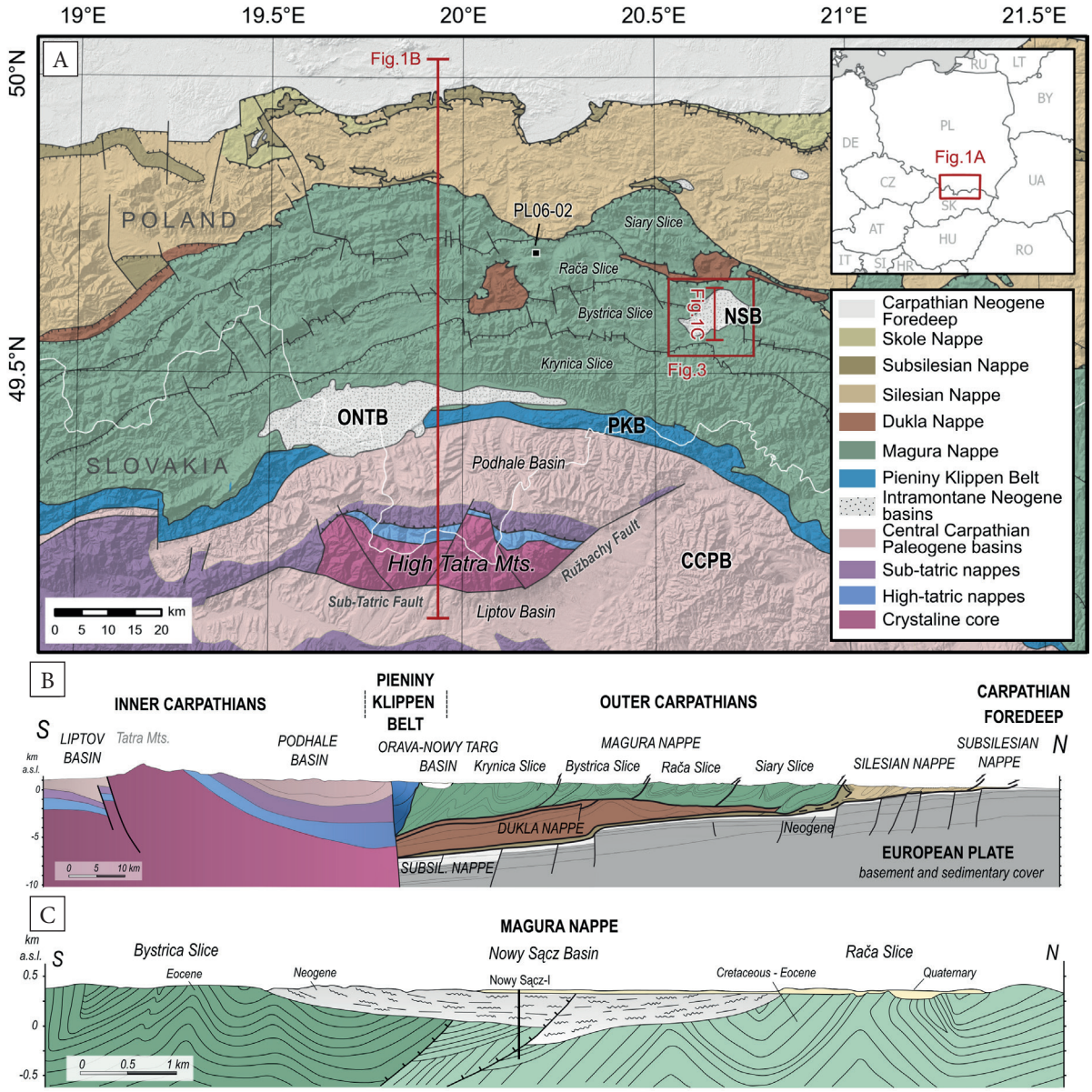

Fig. 1. *Geological setting of the northern part of the Western Carpathians: A) tectonic map after Żytko et al. (1989) and Bezák et al. (2011); B) geological cross-section of the study area after Sikora et al. (1980), Birkenmajer (1985), Oszczypko (2006) and Golonka et al. (2019); C) cross section across the Nowy Sącz Basin after Oszczypko and Wójcik (1992) and Oszczypko-Clowes et al. (2009)*

They are well-dated by fossils from the late Badenian to Sarmatian (nannoplankton zone NN6–NN7) (Oszczypko-Clowes et al. 2009) (Fig. 2). This basin fill was weathered and possibly eroded in the Pliocene to Quaternary when fluvial clastics, delta and slope deposits covered the basin.

The NSB is superimposed on the folded slices of the Magura nappe composed of Albian to Early Miocene flysch sediments (Oszczypko 2006). The youngest formation in the Magura nappe, the flysch deposits are interpreted as filling a piggy-back basin, itself deposited onto the already folded Paleogene to Early Miocene rocks. The youngest formation below the NSB is the Zawada Formation, whose age is Early Miocene, filling completely or partially the NN2 nannoplankton zone (Fig. 2) (Oszczypko et al. 1999). In the other parts of the Magura nappe, around the ONTB and the Pieniny Klippen Belt, the Stare Bystre and Kremna formations have similar Early Miocene stratigraphic

positions (Fig. 2) (Cieszkowski 1992, Oszczypko & Oszczypko-Clowes 2012, Kaczmarek et al. 2016, Oszczypko et al. 2018). Just north of the NSB, a tectonic window exposes the Dukla unit, a deeper nappe pile of the Outer Carpathian nappe package (Fig. 3) (Ślączka et al. 2006).

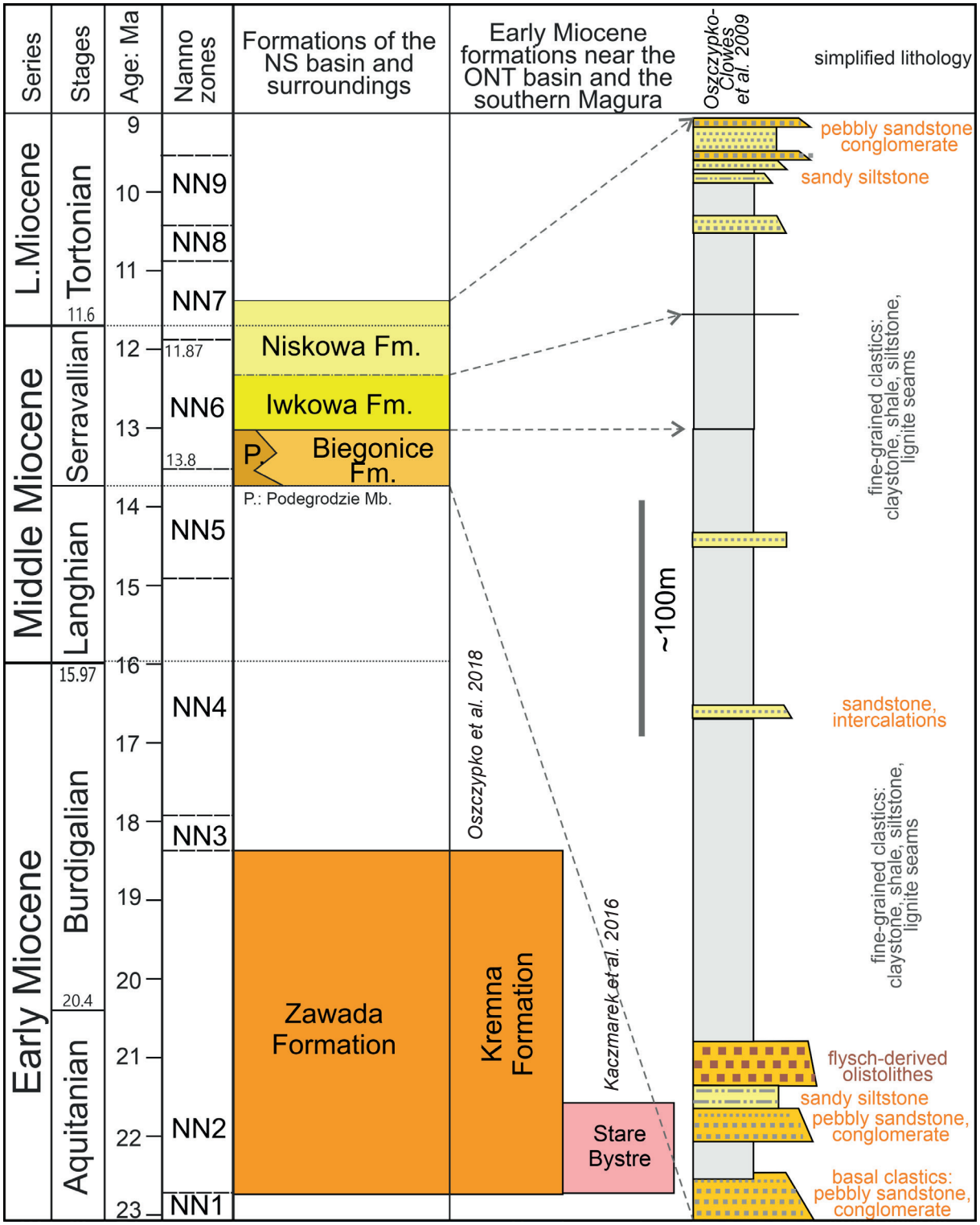

Fig. 2. *Miocene stratigraphy of the formations in and around the Nowy Sącz Basin. Note the lithological column, simplified after Oszczypko-Clowes et al. (2009). Ages of Early Miocene formations are after Oszczypko et al. (1999), Kaczmarek et al. (2016), and Oszczypko-Clowes et al. (2018)*

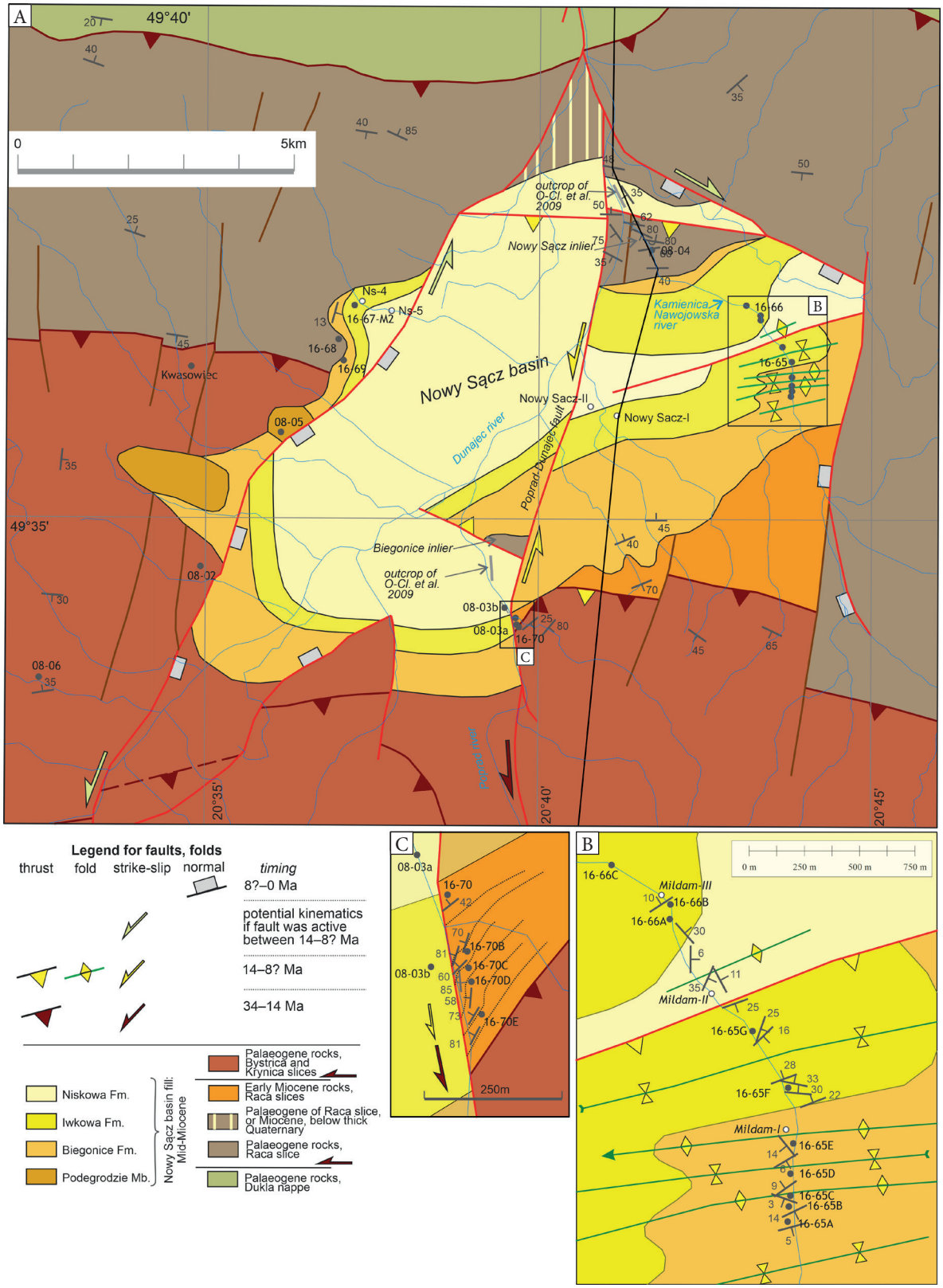

Fig. 3. *Uncovered geological map of the Nowy Sącz Basin without Quaternary deposits: A) the complete area; B) detailed map near sites PL16-65 and PL16-66; C) detailed map near sites PL08-03 and PL16-70. Formation boundaries and faults data are partly after Oszczypko-Clowes et al. (2009) but reinterpreted and completed in this study. Note that due to scarce outcrops, some contacts are hypothetical. Dip data are from Oszczypko and Wójcik (1992), Oszczypko-Clowes et al. (2009) and authors' own observations. Coordinates of the sites are in the Appendix A (attached as a supplemetary file in the online version). Black line indicates the location of section on Figure 8. The letter 'PL' are omitted at the beginning of the site's names for clarity*

The Magura nappe is bounded on the south by the narrow zone of the Pieniny Klippen Belt (PKB) which represents a complex nappe pile overprinted by transpressional deformation in its later stage of evolution (Birkenmajer 1986, Jurewicz 2005, Ludwiniak 2018, Golonka et al. 2019, Plašienka et al. 2020). The Lutetian to earliest Miocene clastic fill of the Central Carpathian Paleogene Basin (CCPB, Fig. 1) potentially represents a forearc basin with respect to the Central Carpathian orogenic arc (Gross et al. 1994, Soták et al. 2001, Garecka 2005). The Paleogene sediments south of the CCPB were deposited onto the eroded surface of the pre-Cenozoic rocks of the Central Western Carpathians assembled during the Late Cretaceous orogeny (Plašienka 2018). This nappe pile is exposed in the High Tatra Mts. (Jurewicz 2005) surrounded by Paleogene formations (Fig. 1). The exhumation of this nappe stack has been determined as Miocene by means of low-temperature thermochronological data (Anczkiewicz et al. 2013, 2015, Králiková et al. 2014, Śmigielski et al. 2016).

METHODS AND DATA SOURCES

Fault-slip data were collected during several field seasons in 2006, 2008, 2010, 2015 and 2016 (coordinates are in Appendix A, appendices are attached as supplementary files in the online version of the article). Both Miocene and Palaeogene–Early Miocene rocks were studied, the latter being observed just near the Middle Miocene sediments, along the southern and western basin margins (Fig. 3). In the interpretation we also used data sets of fractured pebbles and deformation bands from earlier works (e.g., Tokarski et al. 2006), which were compared to the data from this study. One of the formerly studied sites is found near Gruszowiec which is farther from the NSB, but the observed brittle elements, mainly deformation bands and veins, were described in detail (Tokarski & Świerczewska 1998), a comparison of two different approaches of fracture analyses captured the brittle deformation history better. A selection of dip data from geological maps (Oszczypko & Wójcik 1992), and also from publications (Oszczypko-Clowes et al. 2009) are indicated but a complete data set of dip data is beyond the scope of the present work.

Joint, veins, deformation bands, fractured pebbles, faults without or with striae were used to estimate and sometimes calculate the paleostress axes which characterised the brittle deformation. For the estimation of stress axes, fractures were compared to idealized conjugate Mohr-type fracture set of Anderson (1951). For stress tensor calculation, the method of Angelier (1984) was applied, like for the representation of data on stereonets. Fold axes permitted the derivation of shortening direction, assumed to be perpendicular to them. The quality of the database is not excellent, with a few sites resulting in well-constrained stress tensors but in other cases only the estimation of stress axes was possible.

We extensively used the tilt test of the measured brittle elements (Fig. 4). During this back-tilting process we assumed that conjugate fractures have a vertical symmetry plane. If this symmetry plane is vertical (or horizontal) before or after the tilt (after or before the back-tilting of the data set), the fractures are supposed to form at horizontal or actual (tilted) position of beds, respectively. Figure 4A shows an example when the symmetrical normal fault planes with vertical symmetry plane is accepted as post-tilt deformation instead of pre-tilt fracture sets including vertical faults with highly obliques striae: dip-slip striae were preferred with respect to oblique-slip striae because back-tilted fault planes became sub-vertical (Fig. 4A, case 3). On Figure 4B, strike-slip striae were preferred with respect to oblique striae on sub-vertical fault planes (case 1 with respect to case 3). The tilt-test for a single fracture set is not always conclusive (see steep faults in Figure 4B, case 1) but the entire fracture system may provide evidence for pre- or post-tilt nature of fractures (Fig. 4B, case 3). In the case of Figure 4C, dip-slip normal faulting in pre-tilt position shows more symmetry than highly oblique-slip on thrusts of the post-tilt position (case 3 versus case 1); in this case the interpretation could be twofold, but we preferred case 3 (pre-tilt fractures).

Figure 4D shows a case study when progressive back-tilting was applied to currently sub-vertical faults having oblique striae (case 1); the back-tilting of 55° resulted in low-angle thrusts with dip-slip striae while the back-tilting of 70° already resulted in very low dip (case 2, two lines on Figure 4D). The complete back-tilting resulted in normal faults with dip-slip striae but with moderate dip (lower than the expected 60° dip); these two solutions were rejected (Fig. 4D, case 3).

This tilt test was applied to separate deformation episodes within the same stress regime or deformation phase: they are shown separately on the figures. The pre-, syn-, and post-tilt fracture sets (episodes) were grouped into a coherent deformation phase if the geometry, kinematics and stress axes were similar (Figs. 5, 6, and Appendices B, C). The separation and presentation of such pre- syn- or post-tilt episodes sheds light on the coaxial or non-coaxial nature of the deformation. In the extended database (Appendices B, C) we show the data sets separately if two measurement campaigns were carried out; the unified data sets are also shown alike on the Figures 5 and 6.

The relative chronology of the phases was mainly established on the basis of the crosscutting relationship, the reactivation of a given fracture plane by newly formed striae, and on the relative timing of fracture formation with respect to the tilting of beds. This relative chronology is often present between stress regimes (episodes) but sometimes even between phases (these data are marked on Figures 4 and 5 by blue arrows). The other very important chronological criteria are in the pre-Middle Miocene flysch rocks, their folding pre-dates the late Middle Miocene or younger basin sediments. Thus, a pre-tilt fracture set in the flysch rocks has an Early Miocene or older age and has no bearing on the NSB formation. On the other hand, a fracture set having been formed in nearly the present-day dip of the flysch rocks could predate or postdate the onset of NSB sedimentation. As yet, the classification of such a fracture set remains ambiguous.

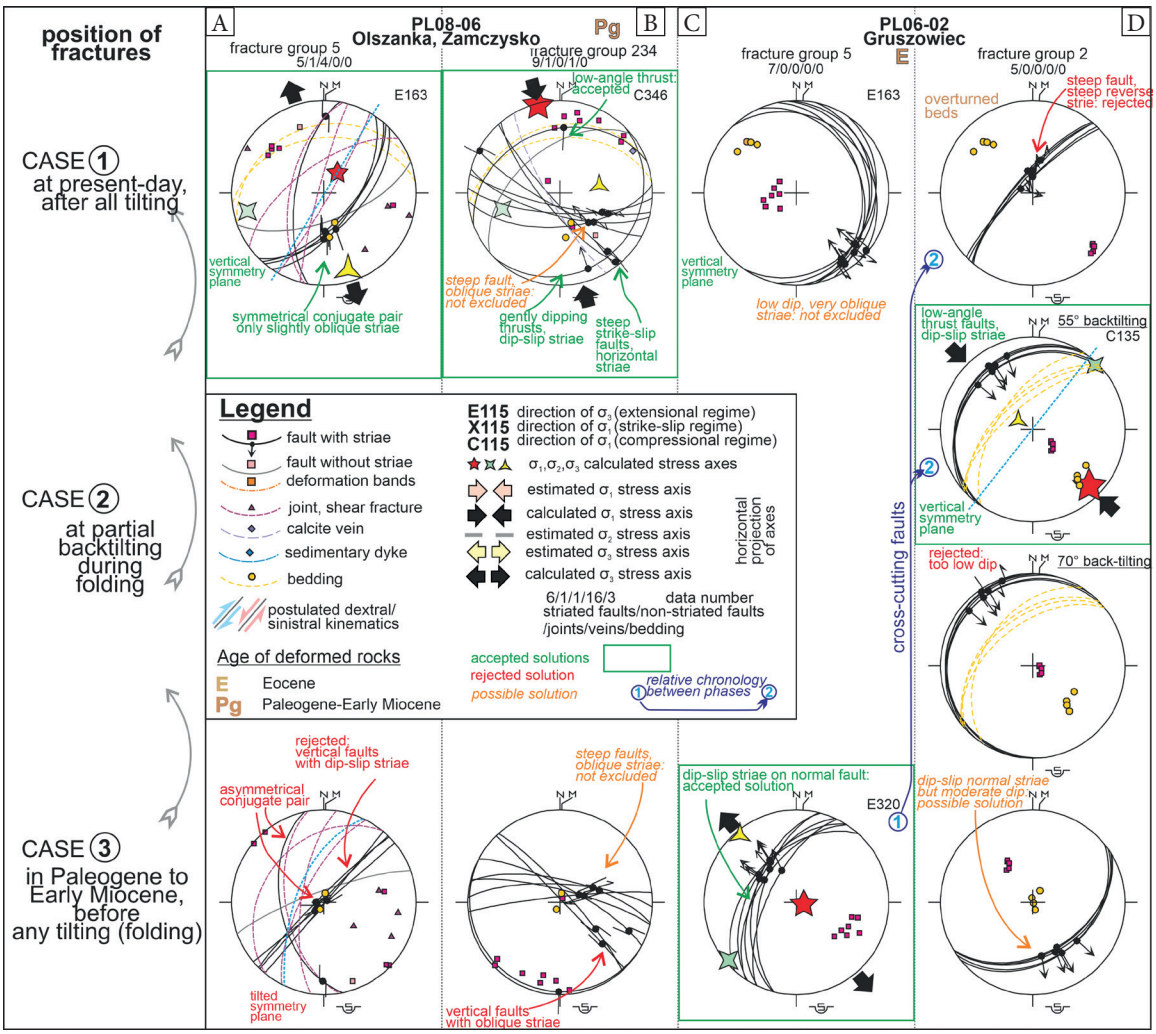

Fig. 4. *Tilt test of stereograms, showing the geometries which support or reject certain fracture sets at a given position. Tilt test is not always conclusive leaving the possibility of both pre- or post-tilt formation of some fractures. Blue arrow with numbers marks the relative chronology between the fracture sets of C and D*

RESULTS

Stress field and fracture pattern in and around the Nowy Sącz Basin

We do not intend to give a detailed analysis of the deformation phases which preceded the Middle Miocene sedimentation. However, to depict a more complete deformation history, we briefly summarise our observations for pre-Middle Miocene deformation phases.

D1 phase: N–S to NW–SE extension

In a few sites, an extensional stress field was calculated or estimated, the direction of extension is between N–S and NW–SE (Fig. 5). The fractures show features typical for early deformation in an incompletely lithified rock: beds are plastically dragged near faults, which evolved from deformation bands, and striae represent stretched minerals. Fault traces are highly curved and show branch points. At site PL08-06, sandstone dykes occur which also demonstrate deformation of weakly lithified rocks. The symmetry plane of conjugate fracture set is perpendicular to layering, and the tilt test could bring them to a horizontal bed position (Fig. 4C). This observation, and the weakly lithified character of the deformed layers, suggests that the deformation occurred just after the deposition while still in a horizontal bed position (Fig. 4). Because of this "early" relative age of deformation, the age of the fracture set changes with the age of the given outcrops and in the two observed cases it could be late Paleogene.

The following observations suggest putting the D1 fracture system as the first D1 deformation phase:

- All fractures show features typical for early "syn-diagenetic" deformation.
- Fractures are symmetrical to bedding and seem to predate the tilt (folding) of the flysch rocks.
- At site PL06-02, the pre-tilt normal faults are cut by thrust faults which are sub-vertical in the present day but were formed during the folding (Fig. 4C, D).
- The successive NW–SE to NNW–SSE compression marks the D2 phases with pre- and post-folding deformations stages.

If D1 was not the oldest phase, the only timing would be the insertion of extension during the folding (between the D2a and D2b–D2c events, see next chapter).

D2 phase: NW–SE to NNW–SSE compression

Palaeogene to Early Miocene beds were folded during the D2 phase, which was a compression of N–S to NW–SE (Fig. 5, Appendix B). This deformation phase is further subdivided into three episodes, the D2a, D2b, D2c are pre- syn-, and post-folding episodes. The deformation was broadly coaxial (Fig. 5B, C), and only at site PL08-06 one can observe a small switch of the maximal stress axes during the folding. However, at present the limited data does not permit a firm conclusion.

Major structures are WSW–ENE to NE–SW striking low-angle reverse faults. At site PL08-03 these are north-dipping shear fractures and striated faults, while at site PL06-02 striated deformation bands were reconstructed by tilt test and represent the D2a episode in tilted Paleogene beds (Figs. 4D, 5B, C). NNE-striking sinistral and NW-striking dextral faults occurred after the folding because they fractured and distorted steep beds.

Beds indicate folding on map scale and outcrop-scale folds were observed along the Poprad River (D2b stage, Fig. 5). At site PL16-70 NW-striking joints and calcite veins might represent cross-fold extensional fractures perpendicular to the folds (*sensu* Aleksandrowski 1989, Tokarski & Świerczewska 1998, Oszczypko & Zuchiewicz 2000) and thus belong the D2b stage.

In site PL06-02, a complex evolution of contractional deformation can be revealed by analysis of the deformation bands. The deformation history was reconstructed using the geometry and deformation mechanism of the bands (Świerczewska & Tokarski 1998, Tokarski et al. 2006), fault-slip analysis completes this picture (Figs. 4D, 5C). Stress calculations are possible due to the presence of striations on the deformation band surfaces. These striae are formed by stretched minerals and not by calcite fibres, indicating early formation before complete lithification. Such a lineation can be present on the surface of deformation bands with minor cataclasis (Beke et al. 2019): using their terminology, we refer deformation band faults to these structures. Some of them resemble soft striae which is also a sign of pre-lithification slip. Three different tilt tests were performed reconstructing the position of fractures at three stages of folding.

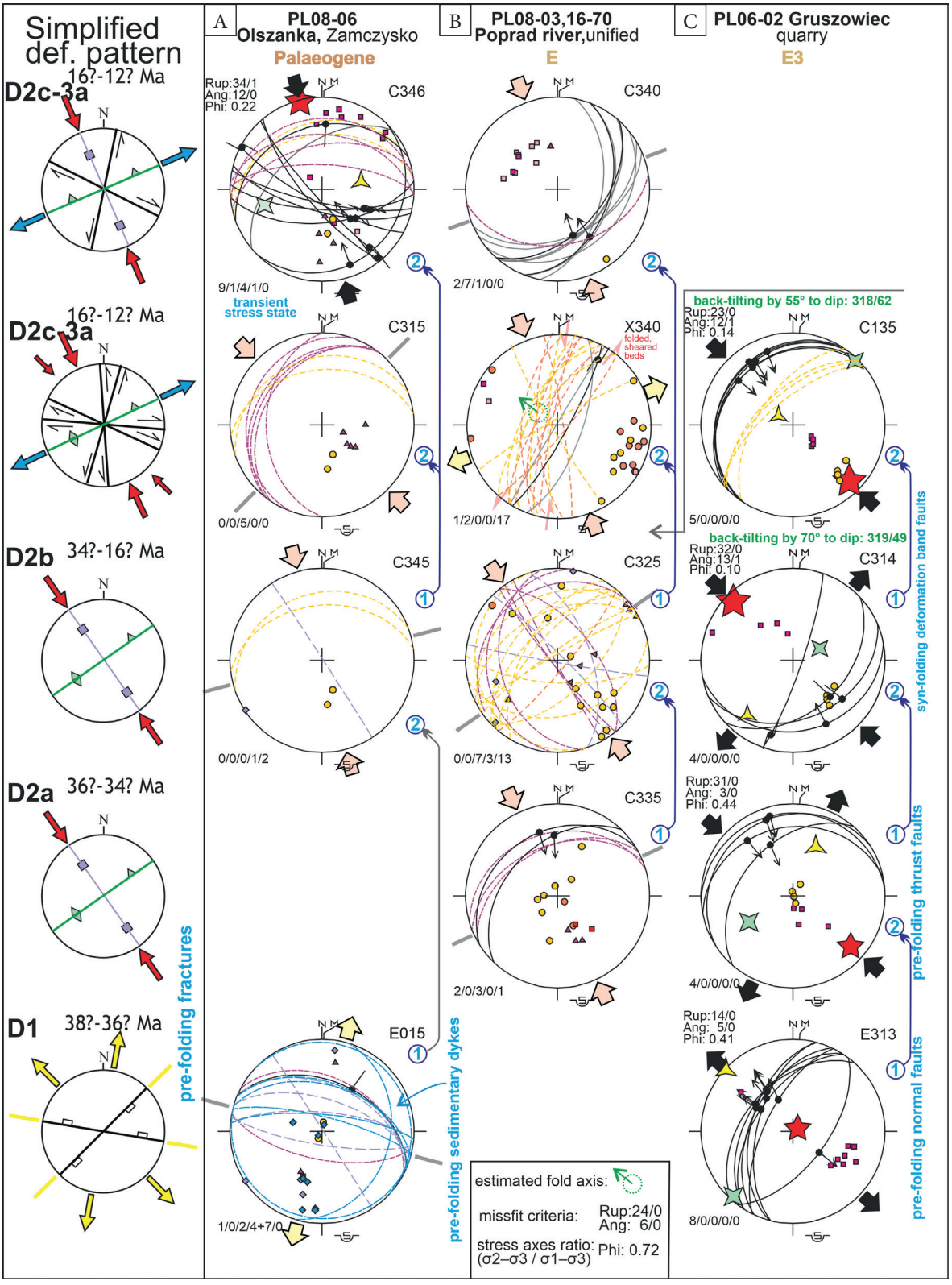

Fig. 5. *Stereograms of fracture sets, bedding data, and interpretations of paleostress axes measured exclusively in Palaeogene rocks and classified as pre-11 Ma deformation phases. The legend for stereograms is in Figure 4. The fracture sets of the transitional D2c–D3a episode are shown in two rows in order to show the variability of fractures and the steeply dipping fold axis in site PL08-03, PL16-70. They post-date folding but their relative chronology is not clear. Misfit criteria RUP and ANG refer to average value of resolved shear vector on the fault plane and the angular deviation of measured and ideal computed striae on the fault plane (Angelier 1984). Blue arrow with numbers marks the relative chronology between the fracture sets*

Three different stages of reverse faulting could be observed, one formed in a horizontal bed position belonging to the D2a episode, while two others were formed during the folding (Figs. 4D, 5C, Appendix B). All of these deformations show coaxial evolution within the same stress field.

This stress field characterizes the contractional deformation of the Magura nappe system. As pointed out by Świerczewska and Tokarski (1998), Tokarski and Świerczewska (1998), Tokarski et al. (2006), and supported by these observations, the folding started at an early stage of lithification, at shallow burial. While the youngest deposits of the nappe units range up to the Early Miocene (broadly 19 Ma, NN2 nannoplankton zone) (Oszczypko et al. 1992, Oszczypko-Clowes et al. 2009), the folding and related shortening might have lasted up to ~18 Ma or even slightly younger, maybe even up to the Middle Miocene.

D2c to D3a deformation

In all pre-Middle Miocene sites, the folding (tiling) of the beds was followed by contractional deformation features. This includes shear fractures (PL08-06), striated faults (PL08-06, PL16-70), all indicating NNW–SSE compression. In these sites tilt test demonstrate that fractures formed after the tilting of the layers in the present-day position (Fig. 4) so they could be classified as D2c deformation episode, just terminating the D2 deformation phase (Fig. 5). However, their temporal relationship with respect to deformation of the Middle Miocene sediments (D3 phase) cannot be judged. So, their classification to an early stage of the late Middle Miocene deformation cannot be excluded. This is the reason that these fractures are marked as uncertainly classified features and assigned to D2c or D3a deformation stage.

One prominent example of this deformation stage is the distortion of already steeply dipping beds along the Poprad River (PL08-03, PL16-70, Fig. 3C). These folds have limb with "averaged" strike of the flysch rocks, which turn to closely N–S striking direction (Fig. 3C). Few striated fault planes can be connected to this vertical-axis folding (Fig. 5B, fracture sets D2c–D3a, Appendix B). All these features are compatible with sinistral shearing and drag folding of an already deformed (folded) package. This shearing could have induced counterclockwise rotation of all elements. Few shear fractures indicating ca. E–W compression can represent those features which were rotated along with beds in counterclockwise direction (Appendix B, site PL16-70). Such "irregular" maximal stress axis was also deduced from joints in nearby outcrops (Oszczypko & Zuchiewicz 2000). All these features, the fractures, distorted beds and dragged folds are outcrop-scale expression of the roughly N–S striking Poprad-Dunajec Fault depicted in earlier maps and studies (Fig. 3) (Oszczypko & Zuchiewicz 2000, Oszczypko-Clowes et al. 2009). We tentatively suggest that this sinistral fault could be associated with thrusting of the Bystrica slice rocks over the Burdigalian formations of the underlying Raca unit; this thrust is depicted on the map (Fig. 3), based on Oszczypko-Clowes et al. (2009).

According to the reconstructions by Oszczypko and Zuchiewicz (2000) and Oszczypko-Clowes et al. (2009) the last folding episode of the Magura nappe could happen in the Early Miocene, after the termination of the Burdigalian sedimentation, after ~19 Ma. Because all flysch formations are dipping more steeply (or are even overturned) than the Middle Miocene basin fill, the folding of the youngest Early Miocene rocks are older than 14 Ma. The ambiguously classified post-folding D2c–D3a stage is younger than the folding of the flysch units and older than the folding of the NS Basin fill, but the upper time constraint cannot be set exactly. The proposed time span is 16–13 Ma.

D3 phase: Middle Miocene or younger phases

This phase is subdivided into three episodes, using temporal relationship with respect to local tilting of the deformed beds, these are the pre-, syn- and post-tilt events (D3a, D3b, D3c). While reverse faults were sometimes clearly connected to tilting of the layers, most of them are classified in the D3b stage (Fig. 6, Appendix C).

The major structural feature is the mild but pronounced tilt of the Middle Miocene strata. Along the southern margin the dip reaches 40–45° (Oszczypko & Wójcik 1992) while an outcrop in the northernmost part shows the south-westerly dip of 30° (Fig. 3) (Oszczypko-Clowes et al. 2009). In the central-northern NSB we made two sets of observation in the Kamienica Nawojowska River.

We found frequent changes in dip direction, from south to north, depicting folds in ~50–200 m wavelength. Shorter wavelength folds were directly observed (Fig. 7A, C). Dip on limbs of the folds do not exceed 35°, generally 10–20°. Constructed fold axis is sub-horizontal and trending E–W (Fig. 3B, Appendix C). Varying dip values and directions and thus the presence of folding was observed along the Kamienica Nawojowska River by Oszczypko-Clowes et al. (2009) (although fold axes were not calculated). They measured steeper dip values (up to 50°) than we did, and this might be due to better outcrop conditions, or to the differences in the classification of the elements: in our data sets moderately dipping planar features were often considered as fractures and not bedding planes (Fig. 7B, F, G). The alternation of different Miocene formations along the river documented by detailed paleontological observations also support the presence of folding (Oszczypko et al. 1992, Oszczypko-Clowes et al. 2009). Tokarski et al. (2006) also noted folding in the western basin margins due to NW–SE compression (site PL08-05 Gostwica, Na Kocie, Fig. 6C). It is to add that Oszczypko (1973) and Oszczypko and Wójcik (1992) already depicted folding of the entire basin fill, in a form of a synform.

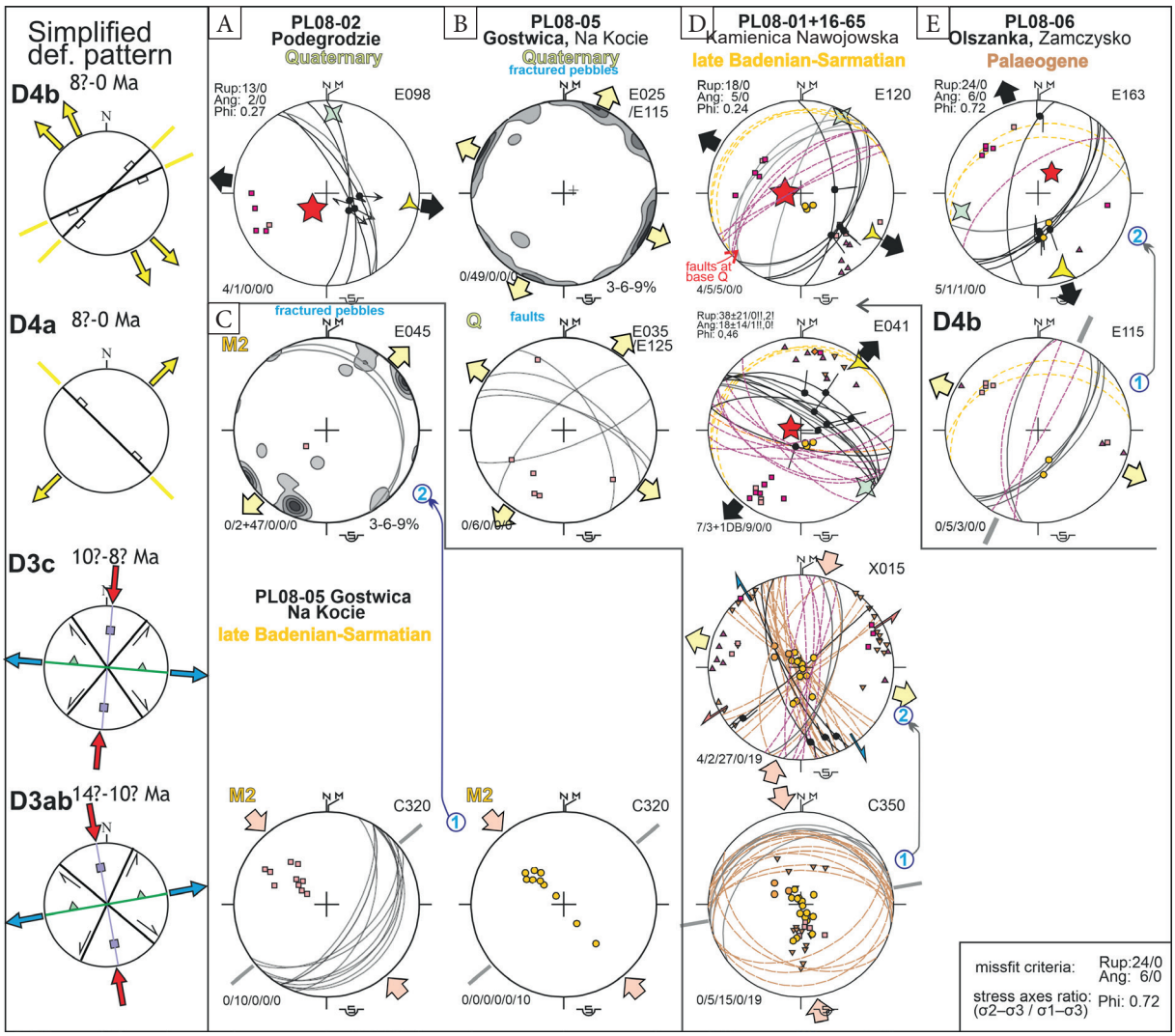

Fig. 6. *Stereograms of fracture sets, bedding data, and interpretations of paleostress axes measured in Middle Miocene to Quaternary but also in Palaeogene rocks. The legend for stereograms is on Figure 4. Data from site PL08-05 are from Tokarski et al. (2006). In site PL08-06 two subsets of fractures belong to the D4b stress regime. Note that site PL08-05 contains both Miocene and Quaternary sub-sites and they are shown in two columns as Figure 6C. Poles of fractures in pebbles are shown by isolines of 3%, 6%, and 9% of data. Blue arrow with numbers marks the relative chronology between the fracture sets*

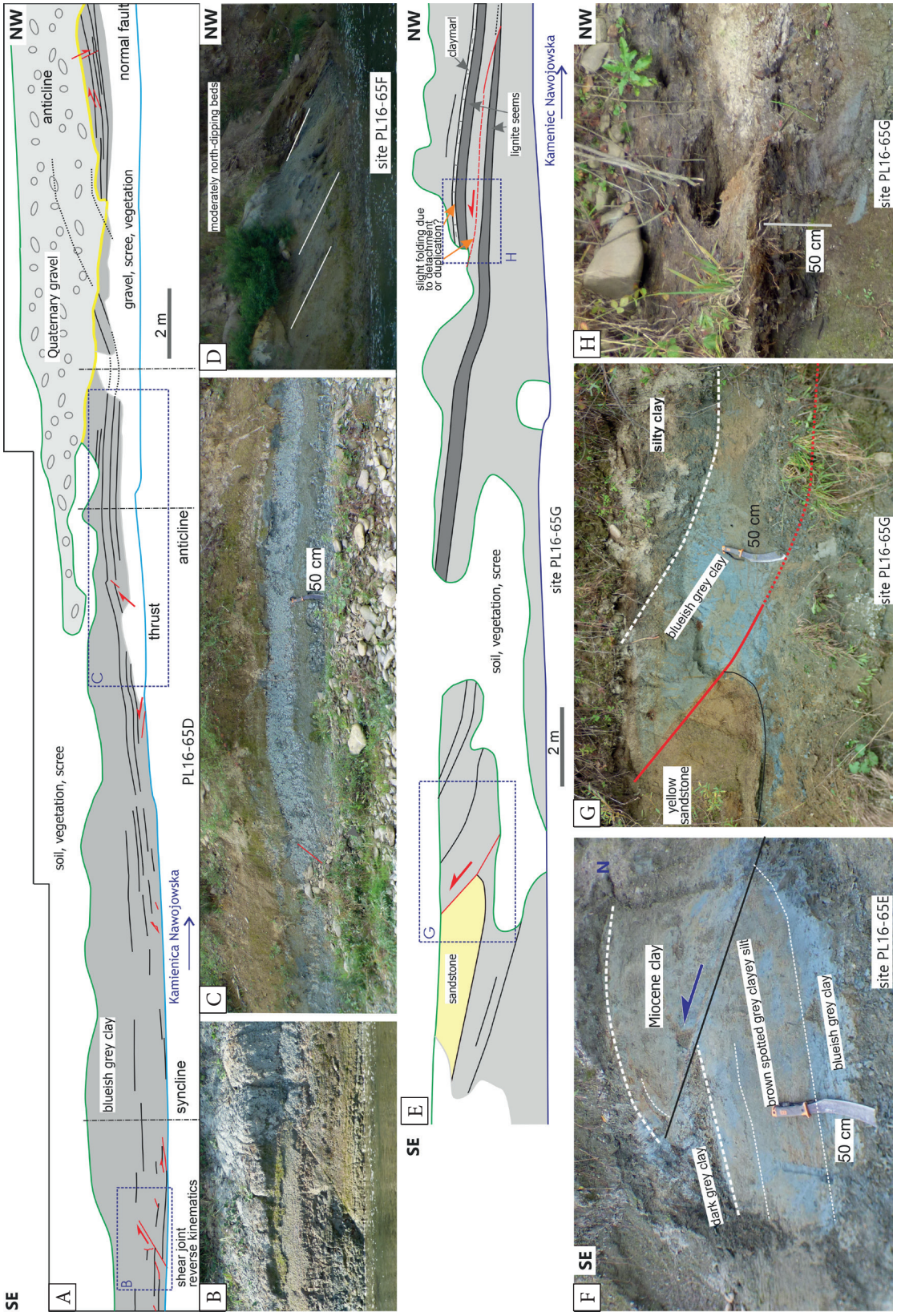

Fig. 7. *Outcrop-scale contractional structures along the Kamienica Nawojowska River (unified sites PL16-65 and PL08-01): A) gentle folds in site PL16-65D; B) detail of thrust-type shear fracture; C) detail of the gentle anticline in blueish grey silty clay; D) moderately dipping layers in site PL16-65F; E) thrust in clay-lignite-sand layers in site PL16-65G; F) thrust fault with drag of the footwall and hanging wall layers; G) detail of the thrust; H) detail of lignite layers, where duplication of lignite could happen by a potential thrust*

In addition to folds, thrust faults were observed in the NSB (Fig. 7B, F, G). Their separation varies from a few cm to a few metres in outcrops. Reverse drag can be associated with displacement (Fig. 7G). Thrusts make a small angle to bedding (10–30°) but occasionally flatten to very low dip and to bedding planes thus forming a flat-ramp geometry (*cf.* Butler 1982). The associated folds can be considered as fault-bend folds, but fault-propagation folds can occur at fault tips (Fig. 7E). Roughly E–W trending low-angle conjugate fractures without visible displacement also have the same geometry as thrusts so they are regarded as shear fractures with potential reverse kinematics. Tokarski et al. (2006) observed NE-striking reverse faults in site PL08-05 (Fig. 6C, Appendix C) where a similarly trending fold axis could be reconstructed. These data show a slightly different compression than in the other sites.

In the NSB the presence of map-scale thrusts is probable because of the distribution of formations. We combined the stratigraphic age of the Miocene beds and their dip direction (Oszczypko-Clowes et al. 2009 and our own data). These data suggest that the younger Miocene formations dip below older Miocene sedimentary rocks along the middle reach of the Kamienica Nawojowska River. The small wavelength of the folds and close spacing of thrusts along the Kamienica Nawojowska River would suggest a common shallow detachment level. The dip of the Middle Miocene layers dip below the northern margin of the Nowy Sącz Paleogene inlier thus we postulate a thrust of older over younger formations (Fig. 3). In the southern basin part, the Biegonice Palaeogene inlier should have had tectonic contact with the youngest Middle Miocene formation (Fig. 3) discovered just south of the inlier (Oszczypko-Clowes et al. 2009): the ESE–WNW strike of the postulated fault would support reverse kinematics. A large thrust was postulated on the cross section of Oszczypko & Wójcik (1992), just below the Nowy Sącz-1 borehole (Fig. 1C) – although Oszczypko-Clowes et al. (2009) suggested a sedimentary origin of the thin Palaeogene intercalation between the Miocene ones.

Strike-slip faults with horizontal striae occur in the NSB (site PL16-65, Fig. 6D, Appendix C). Non-striated shear fractures also seem to form conjugate strike-slip shear fractures (Fig. 6D). The calculated or estimated directions of σ_1 stress axes are almost the same as deduced for gently dipping thrust faults (compare D3b and D3c fracture sets in Appendix C). At site PL08-03 N–S striking joints are perpendicular to fold axes and thrust faults and they could accommodate elongation parallel to the fold axis. These elements seem to form after gentle folding, although the tilt test was inconclusive.

Thus, we consider all of the brittle elements to have been formed in broadly N–S compression and locally E–W extension (Fig. 6). A very slight change (~20°) of the maximal horizontal stress axis in clockwise direction is not excluded between the syn-folding and post-folding deformation stages but the precision and number of data is too small to verify this (compare D3ab and D3c on Figure 6 and Appendix C).

As we noted, the fractures of the uncertainly classified D2c–D3a stage were formed after the folding of the Palaeogene to Early Miocene rocks. They are marked with the same stress field and fracture pattern as those observed in Middle Miocene rocks. These similarities explain why some of the late-stage fractures observed in the flysch rocks can be grouped together with the deformation of the Middle Miocene rocks, into the D3 phase, potentially to the early D3a stage.

As we mentioned earlier, the sinistral Poprad–Dunajec fault (Oszczypko & Zuchiewicz 2000) might have played a role in the deformation of the NSB. While the boundary faults of the Biegonice and Nowy Sącz Palaeogene inliers abut against this cross-basin fault, the sinistral shearing can be coeval with the thrusting along the E–W faults (Fig. 3).

Most of the data indicate fracturing during or after the tilt (folding) of the layers (Fig. 6). This relative chronology data would place the deformation after the deposition of the basin fill, because outcrop-scale syn-sedimentary deformation was not observed. This would suggest that D3 phase occurred certainly in the latest Middle or early Late Miocene: we tentatively suggest 14–8? Ma. However, the origin of the basin will be discussed later.

D4 phase: variable extension between SW–NE and SE–NW

All rock types comprise fractures which imply the presence of an extensional stress field. Preliminarily, we separated two fracture sets which are mutually sub-perpendicular to each other. Striated faults, joints, fractures within pebbles with SE–NW strike form D4a set, while NE–SW striking fractures belong to the D4b set (Fig. 6). In both sets normal faults, (with or without striae) and shear or extensional joints are present (Fig. 6D, Appendix C). Displacement varies from few to 100 cm. The N–S striking striated oblique-slip normal faults (site PL08-02, Fig. 6A) are treated together with NW–SE extensional field because the calculated minimal stress axis (σ_3 = N100E) is closer to stress axis of this fracture set. In the PL08-06 site fractures due to SE–NW extension were probably superimposed by oblique slip dictated by a slight change in extensional stress field with SSE–NNW oriented σ_3 axis (Fig. 6E, Appendix C). We consider this as a local variation of transient character.

Numerous fractures in pebbles belong to both fracture sets, mostly measured in the PL08-05 sites (Fig. 6B, C) (Tokarski et al. 2006). There is no relative chronology between the two fracture sets. In addition, they post-date the tilting, demonstrated in sites PL08-01 and PL08-06. Finally, the similarity between the fracture geometry within pebbles of Miocene and Quaternary age suggest that these fractures are coeval (Tokarski et al. 2006) and belong to a multi- or bidirectional extensional stress field. Bidirectional distribution of normal faults of site PL08-05 strengthen this conclusion (Fig. 6B) (Tokarski et al. 2006). Fractured pebbles of Pleistocene age demonstrate that both the D4a and D4b stress regimes were active during the Quaternary. Similarly, some faults seem to displace the base of Quaternary gravel in site PL16-65 (Fig. 6, Appendix C). However, a latest Miocene or Pliocene onset of the fracturing of the Miocene gravels can neither be excluded nor demonstrated.

Interpretation of the structural geometry of the Nowy Sącz Basin

As we described in the earlier sections, the dip direction is toward the NSB centre, to the N to NW and to the S to SW, on the southern and northern basin margins, respectively. Local deviations occur sporadically: for example, along the western basin margin, the dip is towards the east (Fig. 3). Gentle folds occur at the scale of few tens to 100 m wavelength observed by Oszczypko-Clowes et al. (2009) and by this study. Outcrop-scale thrusts and probable map-scale faults are connected to folds (Fig. 8). All of these features corroborate the contractional structure of the NSB. The synformal geometry of the NSB is shown on the geological cross sections of the published geological map (Oszczypko & Wójcik 1992). Boreholes also corroborate with folded geometry showing much thicker basin fill in the centre (Oszczypko 1973, Oszczypko-Clowes et al. 2009). In addition to the folds, observations on outcrop-scale fracture pattern and deduced stress field estimations support the compressional character of the NSB (Fig. 8). Small-scale thrust faults and conjugate strike-slip faults are marked by N–S to NNW–SSE maximal horizontal stress axis (Figs. 6, 7).

The folding of the basin mostly occurs after the sedimentation of the basin and in this way cannot characterise the origin of the basin. While Oszczypko-Clowes et al. (2009) noted that only the closing of the NSB was marked by shortening, some observations support syn-sedimentary tilting or folding. The NSB has a pronounced asymmetric infill: the oldest terrestrial sequence, the Biegonice Fm, is more than 300 m thick near the southeastern side (Oszczypko-Clowes et al. 2009), but was not observed on the northern side (Figs. 2, 8). The compiled pre-Quaternary map follows Oszczypko-Clowes et al. (2009) that this formation pinches out near Niskowa, thus, only a narrow strip of Biegonice Fm is left on the southern side of the Nowy Sącz Paleogene inlier, but north of it this formation may disappear (Fig. 3). In addition, a 60-meter-thick olistostrome unit was interpreted in the lower part of the basin fill (Nowy Sącz-1 borehole) (Oszczypko-Clowes et al. 2009) which was considered as proof of an active southern basin margin (Figs. 2, 8). This gravity mass flow deposit and the thick asymmetric basin fill can indicate a contractional structure at the southern basin rim: this can be a south-dipping thrust fault or an expressed monocline. Such a basin fill geometry is typical for contractional flexural basins related to thrusting and folding (DeCelles & Giles 1996, Roure 2008) and we propose this geometry for the NSB, too (Fig. 8).

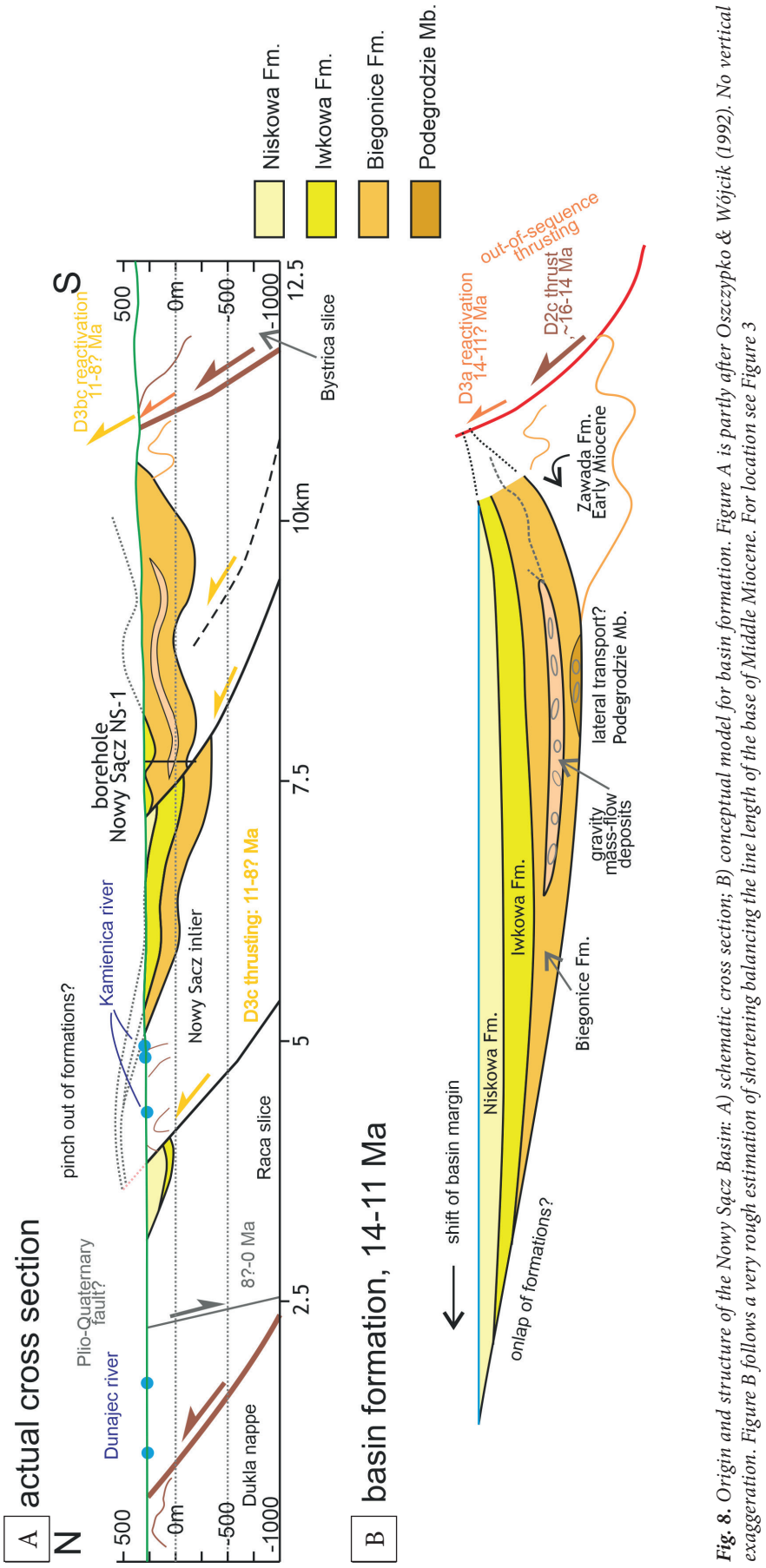

Fig. 8. *Origin and structure of the Nowy Sącz Basin: A) schematic cross section; B) conceptual model for basin formation. Figure A is partly after Oszczypko & Wójcik (1992). No vertical exaggeration. Figure B follows a very rough estimation of shortening balancing the line length of the base of Middle Miocene. For location see Figure 3*

The upward coarsening trend in the Niskowa Formation (Fig. 2) (Oszczypko-Clowes et al. 2009) also characteristic for contractional basin.

The contractional character of the basin and it southern margin is supported by the stress field evolution, there is no major change in the compressional character and in the direction of the maximal stress axes during the entire Miocene. A slight difference might exist between the dominant NW–SE (NNW–SSE) to N–S compression from D2 to D3 phases (Figs. 5, 6, Appendices B, C) but needs further data support. Such a rotation of stress axes, if verified in the future, could be attributed to the counterclockwise rotation of the Magura rock units demonstrated by paleomagnetic data (Márton 2020). A few minor thrusts in the Middle Miocene basin fill can be pre-tilt in relative chronology, and this also indicates that the first increment of deformation was contractional.

On the other hand, the basin is bounded by linear elements along the western and northern margins (Fig. 3). These faults are closely perpendicular to the two determined extensional directions of the post-Middle Miocene stress field. It is thus logical to assume their origin being related to the latest Miocene to Quaternary extension. However, the Middle Miocene initiation of these faults cannot be excluded but in that case their kinematics were different. Namely, the NE-striking western boundary appears to be a sinistral, while the northeastern boundary to represent a dextral fault. This alternative scenario is shown on Figure 3 with separate kinematic signs.

The relationship of the Nowy Sącz Basin to strike-slip faults

A strike-slip related origin can be proposed for the NSB as such models were frequently suggested for the nearby ONTB (Pospíšil 1990a, 1990b, Baumgart-Kotarba 1996, 2001, Pomianowski 2003, Struska 2008, Ludwiniak et al. 2019). In fact, the NSB is cut by the Poprad-Dunajec Fault, along which our data set supported the sinistral shearing proposed by earlier works (Oszczypko & Zuchiewicz 2000). However, this fault cuts through the centre of the basin and does not form a boundary fault (Fig. 3). In addition, the NSB is located north of the Ružbachy Fault, a sinistral transpressional element (Fig. 1) (Sperner et al. 2002). However, along-strike continuity of the Pieniny Klippen Belt and the major thrusts of the Magura nappe exclude the direct connection between the NSB and any southerly located potential sinistral faults.

DISCUSSION

In this part, we will consider the structural evolution of the NSB and surroundings, in terms of structures and stress field. Then we will compare similar observations in the surrounding regions, derived from published works, in order to emphasize the similarities and differences with respect to earlier concepts.

Stress field evolution, comparison with published data

Deformation before the NSB infill

Extensional deformation was observed in Palaeogene rocks (CCPB) near and within the Tatra Mts. by fault-slip analyses and anisotropy of magnetic susceptibility (Sperner et al. 2002, Staneczek et al. 2024). Because it is also a pre-tilt phase, we connect this extension to the D1 pre-tilt phase of this study. Although Sperner et al. (2002) described roughly N–S extension in text, their figures depict variable σ_3 directions (Fig. 9). Our observations of the early diagenetic character of the related fractures also corroborates the suggestion that this extension marked the first deformation. We agree with earlier interpretations that this deformation is related to vertical flattening and an incipient extension during the flysch basin formation itself. This D1 extension seems to have had a very short duration, while it was superimposed by the subsequent compressional D2 phase, which started still in a horizontal bed position. The work of Tokarski and Świerczewska (1998) and Tokarski et al. (2006) suggest that the D2 folding of the flysch units started very early. The mechanism of deformation bands shows that this folding and related fracturing started in a shallow burial position (Świerczewska & Tokarski 1998) and this limits the D2 folding and related fracturing soon after deposition. This timing of D2 folding and

fracturing also suggest that the onset of this phase could vary across the flysch basins, expressed with a diachronous boundary between the D1 and D2 phases (Fig. 9).

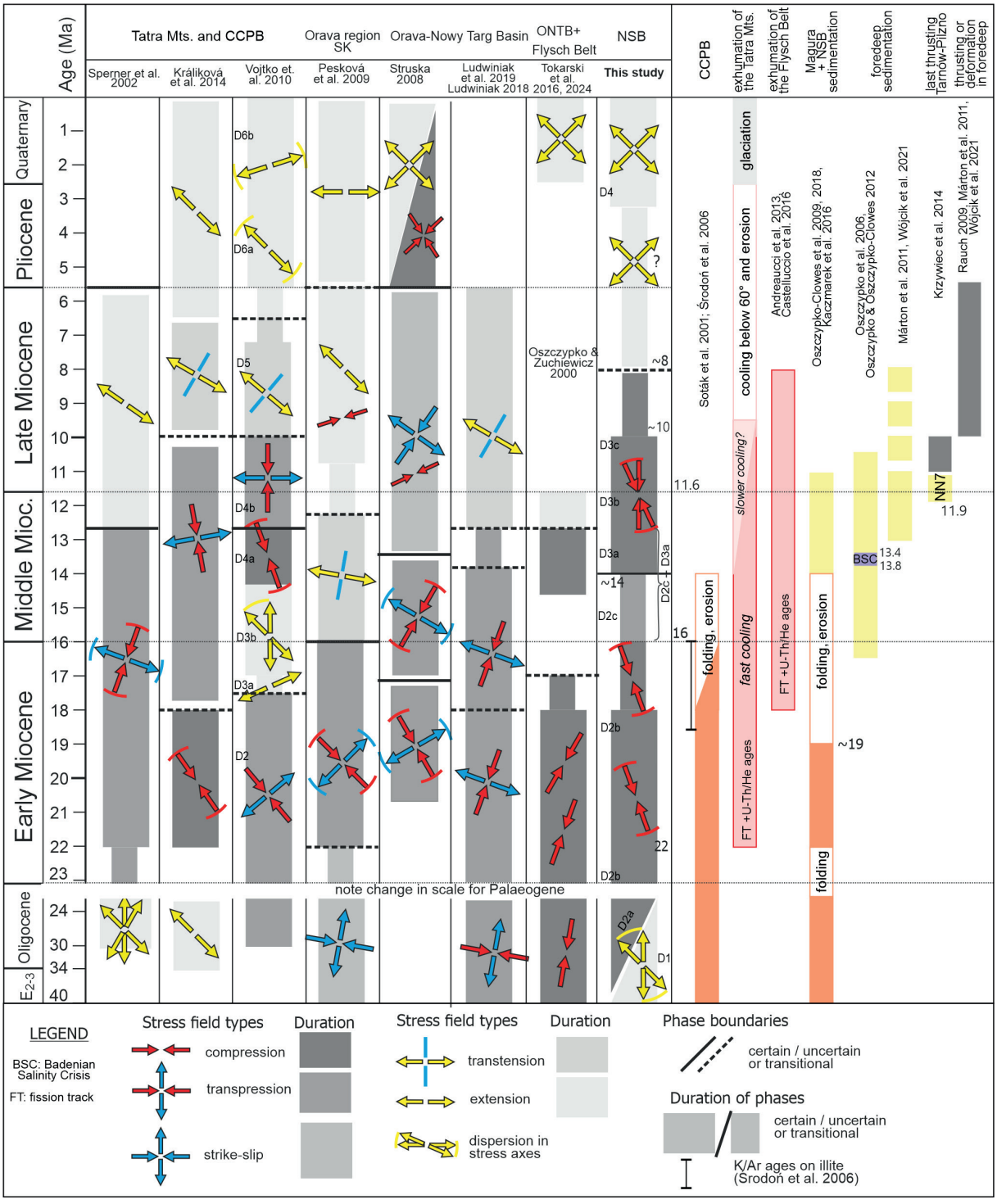

Fig. 9. *Comparison of fault-slip data from the Tatra Mts to those in the Magura nappe, from selected authors. Right-hand side of the figure shows the main sedimentological and tectonic phases from selected publications from the northern Central, Outer Carpathians and foredeep. Phase boundaries are often tentative, when exact age was not precisely known or not defined in the respective works. Local stress state indicated by smaller arrows can occur within a regionally distributed stress field. References see in the text. Note that from the data set for exhumation of the Flysch Belt and Pieniny Klippen Belt (Andreucci et al. 2013, Castellucio et al. 2016) only those are marked which are in the vicinity of the NSB*

D2 folding is the dominant deformation phase in the flysch deposits. The published fault-slip and joint data agree in the compressional or transpressional character of the folding of both the CCPB and Magura nappe (Fig. 9). However, the duration and compressional direction of the folding phase varies slightly among authors. It is due to available time constraints and the exact location of the study. Pešková et al. (2009), Ludwiniak (2018) and Struska (2008) suggested WNW–ESE than later NW–SE compression, in the broad time span of Eocene to Early Miocene. Sperner et al. (2002) and Ludwiniak et al. (2019) determined the maximal stress axis more in the NNE–SSW direction (Fig. 9). Vojtko et al. (2010) determined a transpressional stress field with NW–SE maximal stress axis (Fig. 9). Most of the works consider an Early Miocene timing, after the deposition of the CCPB and Magura sediments.

Our data are partly in agreement with this story: the difference is found in the direction of the shortening and the timing. What we should emphasize, derived from the study of deformation bands (Tokarski & Świerczewska 1998, Tokarski et al. 2006), and the pre-tilt classification of D2a fractures, is the early starting of the folding, shortly after the deposition at a very shallow burial stage. Both the sites PL06-02 Gruszowiec and PL08-03, PL08-06 showed coaxial folding in a compressional setting which could start shortly after the local deposition age and lasted during the formation of the Magura nappe system (Fig. 4) (Tokarski & Świerczewska 1998).

In the Magura nappe a subdivision of this D2 folding phase is possible due to paleontological data and the presence of an erosional hiatus. Namely, the folding was ongoing before, during and after the deposition of the youngest (Early Miocene) flysch-type formation of the Magura nappe, dated as NN2 (~22–19 Ma) (Oszczypko et al. 1999, Oszczypko-Clowes et al. 2009, Kaczmarek et al. 2016). The D2 phase can thus be separated into a Palaeogene–earliest Miocene (~35–22 Ma), an early Miocene (22–19 Ma) and a post-19 Ma folding stages. The upper time constraint of this latter is uncertain, possibly having already stopped around 18 Ma or continuing for a few millions of years more. The last, post-folding contractional episode, the D2c stage, followed the D2b folding, might have happened in the earliest Middle Miocene (Fig. 9). However, the attribution of a given fault-slip data set to these sub-phases cannot be done.

The phase subdivision is slightly different in the CCPB where the youngest preserved sediment belongs to the NN1 nannozone (Garecka 2005). Because the thermal maximum could be reached around 18–17 Ma, as indicated by K-Ar ages on the diagenetic illite, continuous sedimentation could be postulated (Środoń et al. 2006). The major erosion of a several km thick rock pile occurred after ~16–17 Ma and before the onset of ONT and NS basins sedimentation around ~14 Ma. Although this time span is somewhat narrower than in the NSB, the presence of a denudation phase prior to the onset of sedimentation both in the ONT and NS basins can be connected to contractional deformation.

A number of authors attribute a change in the stress field during this intensive deformation in the ONT and NS basins (Fig. 9) (Struska 2008, Pešková et al. 2009, Králiková et al. 2014, Ludwiniak et al. 2019). Vojtko et al. (2010) suggested an extensional phase with roughly NW–SE directed σ_3 (Fig. 9) although this stress field would be different from other regions. However, in the NSB the present study did not find a clear change in stress axes although a slightly transpressional character can be suggested for the D2c stage because of the presence of the Poprad-Dunajec strike-slip fault zone. Also, a slight clockwise change from D2 to D3 is not excluded but remained in the order of 20°. Because this change is close to the error of the method, and because of the noticeable dispersion of individual stress axis determination in both the D2 and D3 phases, this clockwise change is rather a model than clear evidence.

Deformation during the formation of the NSB

Our interpretation is different from other works concerning the structural character of the NS intramountain basin and the stress field which could mark this late Middle Miocene basin formation. Namely, practically all of the works analysing fault-slip data emphasize strike-slip (Struska 2008), transtensional (Ludwiniak et al. 2019), extensional (Pešková et al. 2009) or a locally transpressional regime (Sperner et al. 2002, Králiková et al. 2014)

during the late Middle Miocene. Because the postulated non-compressional origin of the basins is different from the previous folding of the Flysch Belt and also the CCPB, the change in stress field was placed at the inferred onset of basin formation. However, our model favours a compressional origin, the arguments are repeated here: (1) no obvious signs of extensional deformation exist around the NSB (Fig. 6), (2) the activity of strike-slip faulting did not result in the basin subsidence itself, (3) continuous compressional stress observed before and after basin formation, (4) asymmetric basin fill (Fig. 8) is easier to explain in contractional setting, (5) Late Badenian compression was already postulated (Oszczypko & Zuchiewicz 2000). The work of Sperner et al. (2002) described transpressional stress field for the structural elements near the Tatra Mts. The work of Vojtko et al. (2010) described NNW–SSE compression during the late Badenian, which is the time span of sedimentation in the NSB (Fig. 9). A projection of such a compressional or transpressional deformation regime to the NSB is possible and agrees with our contractional model. (The connection of basin formation with the deformation of the Tatra Mts. will be discussed in the subsequent chapter.) Vojtko et al. (2010) extended a compressional or transpressional regime up to the earliest Late Miocene (their phase D4b on Figure 9) and this would correspond to the post-sedimentary contraction observed in the NSB. The late Middle Miocene timing and the extension of contraction up to the earliest Late Miocene would also be in agreement of the exhumation of different Outer Carpathian units constrained by low-temperature thermochronological data (Andreucci et al. 2013, Castelluccio et al. 2016): in our interpretation they indicate the last phase of thrusting.

The stress field evolution seems to be slightly different south and north of the PKB (in the Central and Outer Carpathians). While a clockwise and often gradual change of the maximal stress axis is characteristic in the Central Carpathians (Králiková et al. 2014, Pešková et al. 2009) such a rotation is not obvious in the Magura nappe near the NSB (Oszczypko & Zuchiewicz 2000). The pattern of joints can indicate a slight (~20°) clockwise change of σ_{Hmax} from N–S to NE–SW passing from the innermost to the outermost nappe units, meaning from the older to the younger deformation episodes (Fig. 9) (Oszczypko & Zuchiewicz 2000). This is in line with paleostress changes deduced from fault-slip analyses (Rauch 2013). This change can be connected to the counterclockwise block rotation observed in the Outer Carpathians (Márton 2020).

Deformation after the folding of the NSB infill

Jurewicz (2002) and Jurewicz and Bagiński (2005) determined an ESE–WNW directed extension in the granitic core of the Tatra Mts. The geometry of the striated faults suggests that they post-date the major tilting of the entire Tatra Mts. In their work they attributed this extension to the Sarmatian, but it was probably guided by the postulated timing of the uplift of the Tatra Mts. which was poorly known at the time of publication. In our view it is possible that these fractures are Late Miocene or younger.

The ONTB offer analogies for the D4 extensional deformation. Kukulak (1998), Ahmed and Świerczewska (2013), and Tokarski et al. (2016, 2024) demonstrated a number of sites with fractured pebbles. These fractures can be interpreted as extensional fractures. Poles to fractures have the same double maxima in the ONTB as observed for the NSB, thus, the bidirectional character is similar in both basins (Fig. 9). Baumgart-Kotarba (2001) assumed extensional deformation in the Quaternary while demonstrating thick graben fill within the ONTB.

NW–SE extension was observed by Pešková et al. (2009) in the Orava region in flysch-type sedimentary rocks (Fig. 9). They placed this stress field to the Late Miocene, because they attributed E–W extension to a younger (Pliocene to Quaternary) deformation phase. However, their relative chronology criteria (presence or lack of calcite fibres) can be challenged. Sperner et al. (2002) demonstrated that the roughly N–S compression along the Sub-Tatric fault was overprinted by NW–SE extension (Fig. 9). The chronology is indirect and comes from the observed change from the compressional deformation of postulated Miocene age to the younger, thus Pliocene–Quaternary extension. Králiková et al. (2014) also suggested a similar change from compression to extension through transtensional deformation

episode. Ludwiniak et al. (2019) also emphasized the change from transpressional or strike-slip regime to transtension and they place this change in the Miocene (Fig. 9). The stress field evolution suggested by Vojtko et al. (2010) is probably the most similar to our observation: they described two extensional phases (D6a and D6b on Figure 9), whose minimal stress axes (NW–E and ENE–WSW) almost perfectly match our observation. Post-thrusting extensional deformation was observed by Mazzoli et al. (2010), Andreucci et al. (2013) and reconstructed by balanced cross sections by Casteluccio et al. (2016).

Termination of D3 thrusting and the onset of D4 extension

The onset of the extensional stress regime is difficult to narrow down due to the lack of latest Miocene and Pliocene formations. This might explain why the termination of thrusting and the onset of the extensional stress field varies in the publications (Fig. 9). We tentatively suggest an age around 8 Ma, when major frontal thrusting seems to have vanished in the Polish Outer Carpathians, and a change in stress field is plausible. This imprecise timing would be roughly the same as the Pontian(?) change of stress field in Vojtko et al. (2010). This timing would also be in agreement with the exhumation of different Outer Carpathian units constrained by low-temperature thermochronological data: these vary from ~18 Ma to 8 Ma (Andreucci et al. 2013). Castelluccio et al. (2016) reported 11.6 Ma to 8 Ma apatite (U-Th)/He ages from the Pieniny Klippen Belt. In our interpretation, all these data indicate the last phase of contraction (thrusting and folding) immediately pre-dating the D4 extensional deformation.

On the other hand, the Quaternary duration of the deformation is certain from fractured pebbles and thickness variations (Baumgart-Kotarba 2001, Tokarski et al. 2006, 2024). The focal mechanism of the Podhale earthquake in 2004 (Wiejacz & Dębski 2009) agrees with extensional stress field. All these data demonstrate the activity of this phase in the Quaternary and its extension up to recent time. It is important to note, however, that recent stress fields indicate compression at least along the external thrust front of the Western Carpathians (Jarosiński 2006).

Connection of Middle to Late Miocene deformations of the NSB to wider surroundings

Two major tectonic phenomena mark the evolution of the area: the uplift of the Tatra Mts., and the continuous formation of the Outer Carpathian accretionary wedge (Fig. 9). The timing of the uplift of the Tatra Mts. is well-constrained by thermochronological studies and can be bracketed between ~22 Ma and ~9 Ma (Králiková et al. 2014, Anczkiewicz et al. 2015, Śmigielski et al. 2016). Śmigielski et al. (2016) suggested a faster exhumation before 14 Ma, but the data of Králiková et al. (2014) demonstrates ongoing cooling (and vertical motions) up to 10–9 Ma, at least in the eastern Tatra Mts. In addition, AFT ages from the Podhale region of the CCPB also overlap with this period and extend toward even younger ages of ~8 Ma (Anczkiewicz et al. 2013). Although the onset of exhumation is older than the birth of the NS and ONT basins, this process was ongoing during the formation of both intramountain basins and the post-sedimentary deformation of the NSB (Fig. 9).

The works of Králiková et al. (2014), Anczkiewicz et al. (2015), Śmigielski et al. (2016) discussed the kinematics of the major bounding structure, the Sub-Tatric fault and arrived at the conclusion that reverse faulting is more probable than the exhumation of the footwall of a normal fault, a conclusion already supported by fault-slip analyses and deep seismic profiles (Tomek 1993, Sperner et al. 2002, respectively). However, a normal kinematics of the Sub-Tatric Fault is favoured by other works (e.g., Hrušecký et al. 2002) and used for balanced cross-section construction (Castelluccio et al. 2016).

The formation of the foredeep in the northern periphery of the Outer Carpathians is clearly connected to frontal thrusting (Oszczypko 1998, Gągała et al. 2012, Krzywiec et al. 2012), while triangle zones also developed locally (Krzywiec 2001, Krzywiec & Vergés 2007). The timing is constrained by the basin fill which was considered traditionally as Middle Miocene, but recent works extend this deformation into the earliest Late Miocene (Fig. 9) (Oszczypko & Oszczypko-Clowes 2012, Wójcik et al. 2021). Thus, the last frontal thrusting may be of early Late Miocene

(~11–10 Ma) (Krzywiec et al. 2014) or younger (up to ~8 Ma) (Wójcik et al. 1999, 2021). Additional deformation, including vertical-axis rotation, also affected the foredeep (Rauch 2009, Márton et al. 2011) potentially in a compressive setting (Fig. 9).

The Middle to early Late Miocene time span (16–10 Ma or 16–8 Ma) of the foredeep is very similar to the age of the basin fill of the NSB. Because the post-sedimentary deformation of the NSB is the same in style as the frontal accretion, these deformation elements are part of the same orogen-wide contractional deformation. While the partly coeval Tatra uplift is also compressional, the whole area of the Outer Carpathians and the northern part of the Central Carpathians could be characterised by shortening, including thrusting and folding. In our interpretation, the extensive data set of low-temperature thermochronological data (Andreucci et al. 2013, Castellucio et al. 2016) also corroborate with the final contractional deformation. A quite similar stress field evolution was observed in the eastern CCPB (Vojtko et al. 2010), who emphasized the presence of a continuous compressional or transpressional stress regime up to the middle Late Miocene. Their evolution history is also similar in the potential presence of a small clockwise change in the maximal horizontal stress axis in the latest Middle Miocene (Fig. 9); this would correspond to a change of our D3b to D3c episodes (Fig. 6).

The observed D3 phase contractional deformation postdates the major folding of the flysch belt and can only be coeval with the last stage of frontal thrusting and foredeep deformation. Within-belt mild folding of the former thrust wedge can be considered as "out-of-sequence" deformation, if considering traditional classification. The folding was associated with (continuing) backthrusting near the Tatra Mts.

Assuming the validity of the critical taper model within-wedge shortening indicates changes in the wedge geometry. Wedge widening could probably be due to the fast propagation of the frontal thrust, partly using perfect detachments (evaporates) of the foreland (Krzywiec & Vergés 2007, Krzywiec et al. 2012, 2014). The considerable erosion of folded units could also have contributed to wedge lowering. The mild folding, and particularly the associated thrusting, would have increased the height and decreased the length of the belt. Thus, late Middle Miocene to younger deformation in the Outer Carpathians adds to examples of transient wedges where an increase of wedge height occurred by internal deformation, folding and out-of sequence thrusting.

The fault-slip data and particularly the fractured pebbles indicate a different tectonic scenario after the middle Late Miocene up to recent times. Namely, an extensional stress field could have dominated the NSB and surroundings including the ONTB. Our data set indicates different directions, but the ESE–WNW to SE–NW σ_3 is the most frequently obtained direction, but NE–SW extension might also have been active. Because of the coevality of the D4a and D4b fracture sets, the stress field seems to be a bidirectional extension, close to uniaxial vertical flattening. This type of deformation can be connected to the gravitational collapse of the orogen after the termination of the main thrusting. Although such an evolution is common in orogens, and this scenario was already suggested for the Carpathians (Tokarski et al. 2006), the fault-slip data from around the NSB contribute to such models. Mazzoli et al. (2010), Andreucci et al. (2013) and Castelluccio et al. (2016) interpreted some of the normal faults as being deep-seated and cutting down into the subducted European lower plate. This scenario would indicate a real plate tectonic feature and not simply a gravitational collapse: further works are needed to clarify the driving forces of this extension. In any interpretation, extensional deformation could maintain the exhumation of the High Tatra Mts., but probably not by thrusting but normal faulting and glacial erosion (Tokarski et al. 2012, Szczygieł et al. 2021).

CONCLUSIONS

Fault-slip analysis suggests a persistent contractional deformation during the formation of the studied segment of the Polish Outer Carpathians. In this evolution, the late Middle Miocene Nowy Sącz Basin might also have had a contractional origin, in front of a (reactivated) thrust. This deformation resulted in asymmetric basin fill and gravity mass movements derived from the active southern basin margin. The contraction affected

the slightly indurated basin fill at the same time as the last stage of thrusting in the foredeep. Because of the location of the NSB in the hinterland of the frontal thrusting, its deformation can be considered as a sort of "out-of-sequence" deformation. A comparison with stress field data from the northern Central and southern Outer Carpathians suggests that the entire Early to Middle Miocene could be characterised by compression, although several studies would favour strike-slip related basin formation, mainly around the Tatra Mts. In fact, extensional deformation, probably marked by two interchanging directions, superimposed on the contractional D3 phase, but this occurred only after the frontal thrusting terminated and did not characterise the formation of NSB but only its later deformation. The onset of extension might have been during the latest Miocene or only in the Pliocene–Quaternary and lasted up until recently.

The research was supported by bilateral scientific cooperation between the Polish and Hungarian Academy of Sciences. The finalisation of the analyses was supported by NKFI OTKA project 134873 led by L. Fodor and AGH University of Krakow statutory project 16.16.140.315 (AŚ, PJS). Antek Tokarski introduced us in the field to the problem of the evolution of the NSB, and his help is acknowledged here.

REFERENCES

Ahmed A. & Świerczewska A., 2013. Spękane klasty w żwirach Domańskiego Wierchu (Kotlina Orawska) jako wskaźnik strefy uskokowej – wstępne wyniki badań. [in:] Brzezińska-Wójcik T. (red.), *Neotektonika Polski w świetle dotychczasowych badań: Perspektywy rozwoju: X ogólnopolska konferencja z cyklu „Neotektonika Polski": Lublin, 27–28 września 2013: materiały konferencyjne*, Wydział Nauk o Ziemi i Gospodarki Przestrzennej Uniwersytetu Marii Curie-Skłodowskiej w Lublinie, Lublin, 6–7.

Aleksandrowski P., 1989. Geologia strukturalna płaszczowiny magurskiej w rejonie Babiej Góry [Structural geology of the Magura Nappe in the Mt. Babia Góra region, western Outer Carpathians]. *Studia Geologica Polonica*, 96, 1–140.

Anczkiewicz A.A., Środoń J. & Zattin M., 2013. Thermal history of the Podhale Basin in the Internal Western Carpathians from the perspective of apatite fission track analyses. *Geologica Carpathica*, 64(2), 141–151. https://doi.org/10.2478/geoca-2013-0010.

Anczkiewicz A.A., Danišík M. & Środoń J., 2015. Multiple low temperature thermochronology constraints on exhumation of the Tatra Mountains: New implication for the complex evolution of the Western Carpathians in the Cenozoic. *Tectonics*, 34(11), 2296–2317. https://doi.org/10.1002/2015TC003952.

Anderson E.M., 1951. *The Dynamics of Faulting and Dyke Formation with Application to Britain*. 2nd ed. Oliver & Boyd, Edinburgh.

Andreucci B., Castelluccio A., Jankowski L., Mazzoli S., Szaniawski R. & Zattin M. 2013. Burial and exhumation history of the Polish Outer Carpathians: Discriminating the role of thrusting and post-thrusting extension. *Tectonophysics*, 608, 866–883. https://doi.org/10.1016/j.tecto.2013.07.030.

Andrić N., Sant K., Mąteno L., Mandic O., Tomljenović B., Pavelić D., Hrvatović H., Demir V. & Ooms J., 2017. The link between tectonics and sedimentation in asymmetric extensional basins: Inferences from the study of the Sarajevo-Zenica Basin. *Marine and Petroleum Geology*, 83, 305–332. https://doi.org/10.1016/j.marpetgeo.2017.02.024.

Angelier J., 1984. Tectonic analysis of fault slip data sets. *Journal of Geophysical Research*, 89(B7), 5835–5848. https://doi.org/10.1029/jb089ib07p05835.

Baumgart-Kotarba M., 1996. On origin and age of the Orava Basin, West Carpathians. *Studia Geomorphologica Carpatho-Balcanica*, 30, 101–116.

Baumgart-Kotarba M., 2001. Continuous tectonic evolution of the Orava basin from Late Badenian to the present-day. *Geologica Carpathica*, 52(2), 103–110.

Beke B., Fodor L., Millar L., Petrik A. & Soós B., 2019. Deformation band formation as a function of progressive burial: Depth calibration and mechanism change in the Pannonian Basin (Hungary) *Marine and Petroleum Geology*, 105, 1–16. https://doi.org/10.1016/j.marpetgeo.2019.04.006.

Bezák V., Biely A., Elečko M., Konečný V., Mello J., Polák M. & Potfaj M., 2011. A new synthesis of the geological structure of Slovakia – the general geological map at 1:200,000 scale. *Geological Quarterly*, 55(1), 1–8. https://gq.pgi.gov.pl/article/view/7703.

Birkenmajer K., 1985. Fourth Day. [in:] Birkenmajer K. (ed.), *Carpatho-Balkan Geological Association XIII Congress: Cracow, Poland, 1985, Main geotraverse of the Polish Carpathians (Cracow – Zakopane): Guide to excursion 2*, Wydawnictwa Geologiczne, Warszawa, 90–136.

Birkenmajer K., 1986. Stages of structural evolution of the Pieniny Klippen Belt, Carpathians. *Studia Geologica Polonica*, 88, 7–32.

Butler R.W.H., 1982. The terminology of structures in thrust belts. *Journal of Structural Geology*, 4(3), 239–245. https://doi.org/10.1016/0191-8141(82)90011-6.

Cieszkowski M., 1992. Marine Miocene deposits near Nowy Targ, Magura Nappe, Flysch Carpathians (South Poland). *Geologica Carpathica*, 43(6), 339–346.

Castelluccio A., Mazzoli S., Andreucci B., Jankowski L., Szaniawski R. & Zattin M., 2016. Building and exhumation of the Western Carpathians: New constraints from sequentially restored, balanced cross sections integrated with low-temperature thermochronometry. *Tectonics*, 35(11), 2698–2733. https://doi.org/10.1002/2016TC004190.

DeCelles P.G. & Giles K.A., 1996. Foreland basin systems. *Basin Research*, 8(2), 105–123. https://doi.org/10.1046/j.1365-2117.1996.01491.x.

Fielitz W. & Seghedi I., 2005. Late Miocene–Quaternary volcanism, tectonics and drainage system evolution in the East Carpathians, Romania. *Tectonophysics*, 410(1–4), 111–136. https://doi.org/10.1016/j.tecto.2004.10.018.

Gągała L., Vergés J., Saura E., Malata T., Ringenbach J.-C., Werner Ph. & Krzywiec P., 2012. Architecture and orogenic evolution of the northeastern Outer Carpathians from cross-section balancing and forward modeling. *Tectonophysics*, 532–535, 223–241. https://doi.org/10.1016/j.tecto.2012.02.014.

Garecka M., 2005. Calcareous nannoplankton from the Podhale Flysch (Oligocene-Miocene, Inner Carpathians, Poland). *Studia Geologica Polonica*, 124, 353–370.

Golonka J., Aleksandrowski P., Aubrecht M., Chowaniec J., Chrustek M., Cieszkowski M., Florek R., Gawęda A., Jarosiński M., Kępińska B., Krobicki M., Lefeld J., Lewandowski M., Marko F., Michalik M., Oszczypko N., Picha F., Potfaj M., Słaby E., […] Żelaźniewicz A., 2005. The Orava Deep Drilling Project and the post-Paleogene tectonics of the Northern Carpathians. *Annales Societatis Geologorum Poloniae*, 75(3), 211–248.

Golonka J., Waśkowska A. & Ślączka A., 2019. The Western Outer Carpathians: Origin and evolution. *Zeitschrift der Deutschen Gesellschaft für Geowissenschaften*, 170(3–4), 229–254. https://doi.org/10.1127/zdgg/2019/0193.

Gross P., Filo I., Halouzka R., Haško J., Havrila M., Kováč P., Maglay J., Mello J. & Nagy A., 1994. *Geologická mapa južnej a východnej Oravy 1: 50 000* [*Geological map of the southern and eastern part of Orava*]. Ministerstvo Životneho Prostredia – Geologicky Ústav Dionyza Štúra, Bratislava.

Gruber W., Sachsenhofer R.F., Kofler N. & Decker K., 2004. The architecture of the intramontane Trofaiach pull – apart basin inferred from geophysical and structural studies. *Geologica Carpathica*, 55, 281–298.

Hrušecký I., Pospíšil L. & Kohút M., 2002. Geological interpretation of the reflection seismic profile 753/92. [in:] Hrušecký I. (ed.), *Hydrocarbon Potential of the Eastern Slovakian Basin and Adjacent Areas* [report], Štátny geologický ústav Dionýza Štúra, Bratislava [in Slovakian].

Jarosiński M., 2006. Recent tectonic stress field investigations in Poland: A state of the art. *Geological Quarterly*, 50(3), 303–321.

Jurewicz E., 2002. Geometric analysis of steep-dipping dislocations within the granitoid core in the Polish part of the Tatra Mts. *Annales Societatis Geologorum Poloniae*, 72(1), 89–98.

Jurewicz E., 2005. Geodynamic evolution of the Tatra Mts. and the Pieniny Klippen Belt (Western Carpathians): Problems and comments. *Acta Geologica Polonica*, 55(3), 295–338.

Jurewicz E. & Bagiński B., 2005. Deformation phases in the selected shear zones within the Tatra Mts granitoid core. *Geologica Carpathica*, 56, 17–28.

Kaczmarek A., Oszczypko-Clowes M. & Cieszkowski M., 2016. Early Miocene age of the Stare Bystre formation based on calcareous nannofossils (Magura nappe, outer Carpathians, Poland). *Geological Quarterly*, 60, 341–354. https://doi.org/10.7306/gq.1277.

Králiková S., Vojtko R., Sliva L., Minár J., Fügenschuh B., Kováč M. & Hók J., 2014. Cretaceous–Quaternary tectonic evolution of the Tatra Mts (Western Carpathians): Constraints from structural, sedimentary, geomorphological, and fission track data. *Geologica Carpathica*, 65(4), 307–326. https://doi.org/10.2478/geoca-2014-0021.

Krzywiec P., 2001. Contrasting tectonic and sedimentary history of the central and eastern parts of the Polish Carpathian Foredeep Basin – results of seismic data interpretation. *Marine and Petroleum Geology*, 18(1), 13–38. https://doi.org/10.1016/S0264-8172(00)00037-4.

Krzywiec P. & Vergés J., 2007. Role of the foredeep evaporites in wedge tectonics and formation of triangle zones: Comparison of the Carpathian and Pyrenean Thrust Fronts. [in:] Lacombe O., Lavé J., Roure F. & Vergés J. (eds.), *Thrust Belts and Foreland Basins: From Fold Kinematics to Petroleum Systems*, Frontiers in Earth Sciences, Springer, Berlin, Heidelberg, 383–394. https://doi.org/10.1007/978-3-540-69426-7_20.

Krzywiec P., Bukowski K., Oszczypko N. & Garlicki A., 2012. Structure and Miocene evolution of the Gdów tectonic "embayment" (Polish Carpathian Foredeep) – new model based on reinterpreted seismic data. *Geological Quarterly*, 56(4), 907–920. https://doi.org/10.7306/gq.1067.

Krzywiec P., Oszczypko N., Bukowski K., Oszczypko-Clowes M., Śmigielski M., Stuart F.M., Persano C. & Sinclair H.D., 2014. Structure and evolution of the Carpathian thrust front between Tarnów and Pilzno (Pogórska Wola area, southern Poland) – results of integrated analysis of seismic and borehole data. *Geological Quarterly*, 58(3), 399–416. https://doi.org/10.7306/gq.1189.

Kukulak J., 1998. Charakterystyka sedymentacyjna stropowych osadów stożka domańskiego (neogen/plejstocen) w Kotlinie Orawskiej [Sedimentary characteristics of the topmost deposits, Domański alluvial cone (Neogene/Pleistocene) Orawa Depression, Polish Carpathians]. *Studia Geologica Polonica*, 111, 93–111.

Ludwiniak M., 2010. Multi-stage development of the joint network in the flysch rocks of western Podhale (Inner Western Carpathians, Poland). *Acta Geologica Polonica*, 60(2), 283–316.

Ludwiniak M., 2018. Miocene transpression effects at the boundary of Central Carpathian Paleogene Basin and Pieniny Klippen Belt: Examples from Polish-Slovakian borderland. *Geology, Geophysics, and Environment*, 44(1), 91–110. https://doi.org/10.7494/geol.2018.44.1.91.

Ludwiniak M., Śmigielski M., Kowalczyk S., Łoziński M., Czarniecka U. & Lewińska L., 2019. The intramontane Orava Basin – evidence of large-scale Miocene to Quaternary sinistral wrenching in the Alpine-Carpathian-Pannonian area. *Acta Geologica Polonica*, 69(3), 339–386. https://doi.org/10.24425/agp.2019.126449.

Łoziński M., Wysocka A. & Ludwiniak M., 2015. Neogene terrestrial sedimentary environments of the Orava-Nowy Targ Basin: a case study of the Oravica River section near Čimhová, Slovakia. *Geological Quarterly*, 59(1), 21–34. https://doi.org/10.7306/gq.1209.

Márton E., 2020. Last scene in the large scale rotations of the Western Carpathians as reflected in paleomagnetic constraints. *Geology, Geophysics & Environment*, 46(2), 109–133. https://doi.org/10.7494/geol.2020.46.2.109.

Márton E., Tokarski A.K., Krejči O., Rauch M., Olszewska B., Tomanová Petrová P. & Wójcik A., 2011. 'Non-European' palaeomagnetic directions from the Carpathian Foredeep at the southern margin of the European plate. *Terra Nova*, 23(2), 134–144. https://doi.org/10.1111/j.1365-3121.2011.00993.x.

Mazzoli S., Jankowski L., Szaniawski R. & Zattin M., 2010. Low-T thermochronometric evidence for post-thrusting (<11 Ma) exhumation in the Western Outer Carpathians, Poland. *Comptes Rendus. Géoscience*, 342(2), 162–169. https://doi.org/10.1016/j.crte.2009.11.001.

Nemčok M., Krzywiec P., Wojtaszek M., Ludhová L., Klecker R.A., Sercombe W.J. & Coward P., 2006. Tertiary development of the Polish and eastern Slovak parts of the Carpathian accretionary wedge: In sights from balanced cross sections. *Geologica Carpathica*, 57(5), 355–370.

Nemes F., Neubauer F., Cloetinghh S. & Genser J., 1997. The Klagenfurt Basin in the Eastern Alps: An intra-orogenic decoupled flexural basin? *Tectonophysics*, 282(1–4), 189–203. https://doi.org/10.1016/S0040-1951(97)00219-9.

Oszczypko N., 1973. Budowa geologiczna Kotliny Sądeckiej. *Biuletyn Państwowego Instytutu Geologicznego*, 271–272, 101–197.

Oszczypko N., 1998. The Western Carpathian Foredeep – development of the foreland basin in front of the accretionary wedge and its burial history (Poland). *Geologica Carpathica*, 49(6), 415–431.

Oszczypko N., 2006. Late Jurassic-Miocene evolution of the Outer Carpathian fold-and-thrust belt and its foredeep basin (Western Carpathians, Poland). *Geological Quarterly*, 50(1), 169–194.

Oszczypko N. & Oszczypko-Clowes M., 2012. Stages of development in the Polish Carpathian Foredeep Basin. *Central European Journal of Geosciences*, 4(1), 138–162. https://doi.org/10.2478/s13533-011-0044-0.

Oszczypko N. & Wójcik A., 1992. *Szczegółowa Mapa Geologiczna Polski. 1035, Nowy Sącz. 1:50000*. Polska Agencja Ekologiczna, Warszawa.

Oszczypko N. & Zuchiewicz W., 2000. Jointing in Eocene flysch strata of the mid-eastern Magura Nappe, Polish Outer Carpathians: Implications for the timing of deformation. *Slovak Geological Magazine*, 6(4), 441–456.

Oszczypko N., Stuchlik L. & Wójcik A., 1991. Stratigraphy of fresh-water Miocene deposits of the Nowy Sacz Basin, Polish Western Carpathians. *Bulletin of the Polish Academy of Sciences. Earth Sciences*, 39(4), 433–445.

Oszczypko N., Olszewska B., Slezak J. & Strzępka J., 1992. Miocene marine and brackish deposits of the Nowy Sącz Basin [Polish Western Carpathians] – new lithostratigraphic and biostratigraphic standards. *Bulletin of the Polish Academy of Sciences. Earth Sciences*, 40(1), 83–96.

Oszczypko N., Andreyeva-Grigorovich A., Malata E. & Oszczypko-Clowes M.A., 1999. The lower Miocene deposits of the Rača Subunit near Nowy Sącz (Magura Nappe, Polish Outer Carpathians). *Geologica Carpathica*, 50(6), 419–433.

Oszczypko N., Krzywiec P., Popadyuk I. & Peryt T., 2006. Carpathian Foredeep Basin (Poland and Ukraine): Its sedimentary, structural, and geodynamic evolution. [in:] Golonka J. & Picha, J. (eds.), *Carpathians and Their Foreland: Geology and Hydrocarbon Resources*, AAPG Memoir, 84, The American Association of Petroleum Geologists, Tulsa, Oklahoma, 261–318. https://doi.org/10.1306/985610M843070.

Oszczypko-Clowes M., Oszczypko N. & Wójcik A., 2009. New data on the late Badenian–Sarmatian deposits of the Nowy Sącz Basin (Magura Nappe, Polish Outer Carpathians) and their palaeogeographical implications. *Geological Quarterly*, 53(3), 273–292.

Oszczypko-Clowes M., Oszczypko N., Piecuch A., Soták J. & Boratyn J., 2018. The Early Miocene residual flysch basin at the front of the Central Western Carpathians and its palaeogeographic implications (Magura Nappe, Poland). *Geological Quarterly*, 62(3), 597–619. https://doi.org/10.7306/gq.1425.

Pešková I., Vojtko R., Starek D. & Sliva L., 2009. Late Eocene to Quaternary deformation and stress field evolution of the Orava region (Western Carpathians). *Acta Geologica Polonica*, 59(1), 73–91.

Plašienka D., 2018. Continuity and episodicity in the early Alpine tectonic evolution of the Western Carpathians: How large-scale processes are expressed by the Orogenic architecture and rock record data. *Tectonics*, 37(7), 2029–2079. https://doi.org/10.1029/2017TC004779.

Plašienka D., Bučová J. & Šimonová V., 2020. Variable structural styles and tectonic evolution of an ancient backstop boundary: The Pieniny Klippen Belt of the Western Carpathians. *International Journal of Earth Sciences*, 109, 1355–1376. https://doi.org/10.1007/s00531-019-01789-5.

Pomianowski P., 2003. Tektonika Kotliny Orawsko-Nowotarskiej: wyniki kompleksowej analizy danych grawimetrycznych i geoelektrycznych. *Przegląd Geologiczny*, 51(6), 498–506.

Porkoláb K., Kövér Sz., Benkó Zs., Héja G.H., Fialowski M., Soós B., Gerzina-Spajić N. Đerić N. & Fodor L., 2019. Structural and geochronological constraints from the Drina-Ivanjica thrust sheet (Western Serbia): Implications for the Cretaceous–Paleogene tectonics of the Internal Dinarides. *Swiss Journal of Geosciences*, 112(1), 217–234. https://doi.org/10.1007/s00015-018-0327-2.

Pospíšil L., 1990a. Současné možnosti identifikace střižných zón v oblasti Západních Karpát [The present possibilities of identification of shear zones in the area of the West Carpathians]. *Mineralia Slovaca*, 22, 19–31.

Pospíšil L., 1990b. Tíhové modely oravské neogenní pánve [Gravity models of the Orava Neogene Basin]. *Zemní plyn a nafta*, 35(3–4), 301–307.

Ratschbacher L., Frisch W., Neubauer F., Schmid & Neugebauer J., 1989. Extension in compressional orogenic belts: The Eastern Alps. *Geology*, 17, 404–407. https://doi.org/10.1130/0091-7613(1989)017<0404:EICOBT>2.3.CO;2.

Ratschbacher L., Frisch W., Linzer H. G. & Merle O., 1991. Lateral extrusion in the Eastern Alps. Part 2: Structural analysis. *Tectonics*, 10(2), 257–271. https://doi.org/10.1029/90TC02623.

Rauch M., 2009. Neogene stress field in the central and eastern parts of the outer Polish Carpathian Foredeep. *Geodinamica Acta*, 22(1–3), 145–156.

Rauch M., 2013. The Oligocene–Miocene tectonic evolution of the northern Outer Carpathian fold-and-thrust belt: Insights from compression-and-rotation analogue modelling experiments. *Geological Magazine*, 150(6), 1062–1084. https://doi.org/10.1017/S0016756813000320.

Roure F., 2008. Foreland and Hinterland basins: What controls their evolution? *Swiss Journal of Geosciences*, 101(1), S5–S29. https://doi.org/10.1007/s00015-008-1285-x.

Sachsenhofer R.F., Kogler A., Polesny F., Strauss P. & Wagreich M., 2000. The Neogene Fohnsdorf Basin: Basin formation and basin inversion during lateral extrusion in the Eastern Alps (Austria). *International Journal Earth Sciences*, 89, 415–430. https://doi.org/10.1007/s005310000083.

Sikora W., Borysławski A., Cieszkowski M. & Gucik S., 1980. *Przekrój geologiczny Kraków – Zakopane. 1: 50 000* [*Geological cross-section Cracow – Zakopane*]. Wydawnictwa Geologiczne, Warszawa.

Soták J., Pereszlenyi M., Marschalko R., Milicka J. & Starek D., 2001. Sedimentology and hydrocarbon habitat of the submarine-fan deposits of the Central Carpathian Paleogene Basin (NE Slovakia). *Marine and Petroleum Geology*, 18(1), 87–114. https://doi.org/10.1016/S0264-8172(00)00047-7.

Ślączka A., Krugłov S., Golonka J., Oszczypko N. & Popadyuk I., 2006. Geology and hydrocarbon resources of the Outer Carpathians, Poland, Slovakia, and Ukraine: General geology. [in:] Golonka J. & Picha F.J. (eds.), *The Carpathians and Their Foreland: Geology and Hydrocarbon Resources*, AAPG Memoir, 84, American Association of Petroleum Geologists, Tulsa, Oklahoma, 221–258. https://doi.org/10.1306/985610M843070.

Śmigielski M., Sinclair H.D., Stuart F.M., Persano C. & Krzywiec P., 2016. Exhumation history of the Tatry Mountains, Western Carpathians, constrained by low-temperature thermochronology. *Tectonics*, 35(1), 187–207. https://doi.org/10.1002/2015TC003855.

Sperner B., Ratschbacher L. & Nemčok M., 2002. Interplay of lateral extrusion, subduction rollback, and continental collision in the Tertiary evolution of the Western Carpathians. *Tectonics*, 21(6), 1051–1075. https://doi.org/10.1029/2001TC901028.

Środoń J., Kotarba M., Biroň A., Such P., Clauer N. & Wójtowicz A., 2006. Diagenetic history of the Podhale-Orava Basin and the underlying Tatra sedimentary structural units (Western Carpathians): Evidence from XRD and K-Ar of illite-smectite. *Clay Minerals*, 41(3), 751–774. https://doi.org/10.1180/0009855064130217.

Staneczek D., Szaniawski R., Chadima M. & Marynowski L., 2024. Multi-stage tectonic evolution of the Tatra Mts recorded in the para- and ferromagnetic fabrics. *Tectonophysics*, 880, 230338. https://doi.org/10.1016/j.tecto.2024.230338.

Struska M., 2008. *Neogeńsko-czwartorzędowy rozwój strukturalny Kotliny Orawskiej w świetle badań geologicznych, geomorfologicznych oraz teledetekcyjnych*. AGH University of Science and Technology, Krakow [Ph.D. thesis].

Strzelecki P.J. & Świerczewska A., 2023. Wpływ więźby skały na mechanizm deformacji: studium przypadku wstęg deformacyjnych w piaskowcach otryckich (Bieszczady) [The impact of rock fabric on deformation: A case study of deformation bands in the Otryt sandstone (Bieszczady Mountains, SE Poland)]. *Przegląd Geologiczny*, 71(4), 231–234. https://doi.org/10.7306/2023.20.

Strzelecki P.J., Świerczewska A., Kopczewska K., Fheed A., Tarasiuk J. & Wroński S., 2021. Decoding rocks: An assessment of geomaterial microstructure using X-ray microtomography, image analysis and multivariate statistics. *Materials*, 14(12), 3266. https://doi.org/10.3390/ma14123266.

Szczygieł J., Gradziński M., Bella P., Hercman H. & Wróblewski W., 2021. Quaternary faulting in the western Carpathians: insights into paleoseismology from cave deformations and damaged speleothems (Demänová Cave System, Low Tatra Mts). *Tectonophysics*, 820, 229111. https://doi.org/10.1016/j.tecto.2021.229111.

Świerczewska A. & Tokarski A.K., 1998. Deformation bands and the history of folding in the Magura nappe, Western Outer Carpathians (Poland). *Tectonophysics*, 297, 73–90. https://doi.org/10.1016/S0040-1951(98)00164-4.

Tokarski A.K. & Świerczewska A., 1998. History of folding in the Magura nappe, Outer Carpathians, Poland, [in:] Rossmanith H.-P. (ed.), *Mechanics of Jointed and Faulted Rock*, AA Balkema, Rotterdam, 125–130. https://doi.org/10.1201/9780203747810-17.

Tokarski A., Świerczewska A., Zuchiewicz W., Márton E., Hurai V., Anczkiewicz A., Michalik M., Szeliga W. & Rauch-Włodarska M. 2006. Conference Excursion 1: Structural development of the Magura Nappe (Outer Carpathians): From subduction to collapse. *GeoLines*, 20, 145–164.

Tokarski A.K., Świerczewska A., Zuchiewicz W., Starek D. & Fodor L., 2012. Quaternary exhumation of the Carpathians: A record from the Orava-Nowy Targ Intramontane Basin, Western Carpathians (Poland and Slovakia. *Geologica Carpathica*, 63(4), 257–266. https://doi.org/10.2478/v10096-012-0021-7.

Tokarski A.K., Márton E., Świerczewska A., Fheed A., Zasadni J. & Kukulak J., 2016. Neotectonic rotations in the Orava-Nowy Targ Intramontane Basin (Western Carpathians): An integrated palaeomagnetic and fractured clasts study. *Tectonophysics*, 685, 35–43. https://doi.org/10.1016/j.tecto.2016.07.013.

Tokarski A.K., Świerczewska A., Lasocki S., Cuong N.Q., Strzelecki P.J., Olszak J., Kukulak J., Alexanderson H., Zasadni J., Krąpiec M. & Mikołajczak M., 2020. Active faulting and seismic hazard in the Outer Western Carpathians (Polish Galicia): Evidence from fractured Quaternary gravels. *Journal of Structural Geology*, 141, 104210. https://doi.org/10.1016/j.jsg.2020.104210.

Tokarski A.K., Świerczewska A., Strzelecki P.J., Lasocki S., Olszak J., Alexanderson H., Thamó-Bozsó E., Kukulak J., Mikołajczak M., Krąpiec M. & Furi J.I., 2024. Seismic damage in Quaternary fluvial gravels in low seismicity thrust-andfold belts: Case study of the Outer Western Carpathians (Poland and Slovakia). *Journal of Structural Geology*, 178, 105027. https://doi.org/10.1016/j.jsg.2023.105027.

Tomek Č., 1993. Deep crustal structure beneath the central and inner West Carpathians. *Tectonophysics*, 226(1–4), 417–431. https://doi.org/10.1016/0040-1951(93)90130-C.

Vojtko R., Tokárová E., Sliva L. & Pesková I., 2010. Reconstruction of Cenozoic paleostress fields and revised tectonic history in the northern part of the Central Western Carpathians (the Spisská Magura and Východné Tatry Mountains). *Geologica Carpathica*, 61(3), 211–225. https://doi.org/10.2478/v10096-010-0012-5.

Wiejacz P. & Dębski W., 2009. Podhale, Poland, earthquake of November 30, 2004. *Acta Geophysica*, 57(2), 346–366. https://doi.org/10.2478/s11600-009-0007-8.

Wójcik A. & Jugowiec M., 1998. The youngest member of the folded Miocene in the Andrychów region (Southern Poland). *Przegląd Geologiczny*, 46(8/2), 763–770.

Wójcik A., Szydło A., Marciniec P. & Nescieruk P., 1999. The folded Miocene of the Andrychów region. *Biuletyn Państwowego Instytutu Geologicznego*, 387, 191–195.

Wójcik A., Garecka M.K., Malata T., Pilarz M., 2021. The youngest deposits infilling the Gdów "embayment" (Carpathian orogenic front, south Poland) are not older than late Sarmatian-Pannonian. *Geological Quarterly*, 65(2), 22. https://doi.org/10.7306/gq.1576.

Zuchiewicz W., Tokarski A.K., Świerczewska A. & Cuong N.Q., 2009. Neotectonic activity of the Skawa River Fault Zone (Outer Carpathians, Poland). *Annales Societatis Geologorum Poloniae*, 79(1), 67–93. https://bibliotekanauki.pl/articles/191395.pdf [access: 2.05.2025].

Żytko K., Zając R., Gucik S., Ryłko W., Oszczypko N., Garlicka I., Nemčok J., Eliáš M., Menčik E. & Stránik Z., 1989. Map of the tectonic elements of the Western Outer Carpathians and their foreland. [in:] Poprawa A. & Nemčok J. (eds.), *Geological Atlas of the Western Outer Carpathians and Their Foreland*, Wydawnictwa Geologiczne, Warszawa.

Supplementary data associated with this article (Appendices A, B, and C) can be found in the online version at: https://doi.org/10.7494/geol.2025.51.2.107.

Appendix A. *Coordinates of the observed sites in the NSB and surroundings, in UTM 34 WGS84. Note that the site PL06-02 is shown on Figure 1*

Appendix B. *All data of the phases D1 and D2 and the uncertainly classified D2c–D3a fracture sets: their classifications, estimated or calculated stress axes, and relative chronology data. The D2c–D3a sets are shown in several lines in order to present the variability of data. Misfit criteria RUP and ANG refer to average value of resolved shear vector on the fault plane and the angular deviation of measured and ideal computed striae on the fault plane (Angelier 1984): average values and standard deviations are shown with number of misfit data above threshold. Phi (Φ) refers to the ratio of principal stress axes* σ_2–σ_3/σ_1–σ_3

Appendix C. *All data of the phases D3 and D4, their classifications, estimated or calculated stress axes, and relative chronology data*